NASA CONTRACTOR REPORT

NASA CR-1584

THE DEVELOPMENT OF RADIATION RESISTANT INSULATING LAYERS FOR PLANAR SILICON TECHNOLOGY

by R. P. Donovan, M. Simons, and L. K. Monteith

Prepared by
RESEARCH TRIANGLE INSTITUTE
Research Triangle Park, N. C.
for Langley Research Center

NATIONAL AERONAUTICS AND SPACE ADMINISTRATION • WASHINGTON, D. C. • MAY 1970

NASA CR-1584

THE DEVELOPMENT OF RADIATION RESISTANT INSULATING LAYERS FOR PLANAR SILICON TECHNOLOGY

By R. P. Donovan, M. Simons,
and L. K. Monteith

May 70

Prepared under Contract No. NAS 1-8156 by
RESEARCH TRIANGLE INSTITUTE
Research Triangle Park, N.C.

for Langley Research Center

NATIONAL AERONAUTICS AND SPACE ADMINISTRATION

For sale by the Clearinghouse for Federal Scientific and Technical Information
Springfield, Virginia 22151 – CFSTI price $3.00

FOREWORD

These experiments were sponsored by the Instrument Physics Research Section of FID, NASA Langley Research Center, Hampton, Virginia. C. L. Fales, Jr., was the NASA technical monitor. The contract period extended from May 29, 1968 to June 28, 1969.

Measurements of charge injection and bias-temperature stressing of various samples were made by J. R. Bridges and J. R. Hauser of the Electrical Engineering Department of North Carolina State University, Raleigh, N. C.

It is a pleasure to acknowledge the contribution of H. D. Hendricks, J. S. Heyman and W. Wilser of the Chemistry and Physics Branch of AMPD, Langley Research Center, in performing all ion implantations and to thank B. E. Deal of the Research and Development Laboratory of Fairchild Semiconductor Corporation for providing various oxide samples.

TABLE OF CONTENTS

LIST OF ILLUSTRATIONS

THE DEVELOPMENT OF RADIATION RESISTANT INSULATING LAYERS FOR PLANAR SILICON TECHNOLOGY

R. P. Donovan, M. Simons and L. K. Monteith*
Research Triangle Institute

INTRODUCTION

The advent of MOS transistors dates back to the early 1960's. Their conception and development were described by Attala and Kahng (Ref. 1), Sah (Refs. 2,3) and Heiman and Hofstein (Ref. 4) in a series of papers and presentations between 1960 and 1964. The properties of these transistors were considerably different from the conventional bipolar transistor in that the control electrode was a high impedance electrode and enabled these devices to operate in circuits quite similarly to vacuum tubes. Functions that could be performed with bipolar transistors only with great difficulty could ofttime be performed very cheaply and easily by MOS transistors. Indeed in certain combinations--such as Sah's tetrode (Ref. 2)--the advantages of both the MOS and the bipolar transistor could be combined into one structure. The outlook for device growth never seemed brighter.

Follow-up on these exciting announcements was disappointing. Slowly an awareness of the severe manufacturing problems required by these new devices became appreciated. One entire issue of the IBM Journal of Research was devoted to exploring certain of these problems (Ref. 5). In this atmosphere it is not surprising in retrospect that the recognition of radiation sensitivity problems by Hughes and Giroux (Ref. 6) attracted less attention than it might otherwise have done. Manufacturers throughout the country had cleanliness on their minds and were concerned primarily in eliminating the effects of ions from MOS transistor efforts.

Manufacturing methods have now improved to the point where ion-free devices are commercially available and other problems such as radiation sensitivity are receiving more attention. Again, much of the work has been carried out by workers at Fairchild who also made the major contributions in identifying the role of contaminants in the oxidation process (Ref. 7). The analysis of the effects of ionizing radiation upon the oxide properties has been described chiefly by Snow, Grove, and Fitzgerald (Ref. 8) along with Zaininger (Ref. 9). In Reference 8, Snow, et al., describe the influence of ionizing radiation upon the oxide as causing two primary effects: 1) the creation of a net positive space charge in the oxide, and 2) the introduction of fast surface states at the oxide-silicon interface. Both these effects can cause undesirable MOS device instabilities and cause otherwise satisfactorily operating circuits to drift and malfunction in ionizing radiation environments.

---

* Associate Professor, Electrical Engineering Department, North Carolina State University, Raleigh, N. C. (Consultant at Research Triangle Institute).

The first effect--the creation of a net positive space charge in the oxide--has been recognized for over three years now and is at least partially understood (Refs. 8-10). In the model used to explain the space charge buildup the primary effect of the ionizing radiation is to create hole-electron pairs in the oxide. This interaction is expected between any insulator and ionizing radiation and invokes no special properties of the irradiated oxide--radiation with energy in excess of the oxide band gap (~ 8 eV) is expected to create hole-electron pairs. Once created these excess carriers are expected to recombine and decay back to their equilibrium concentrations which for the oxide (as for all insulators) are very small. Other events may occur to interrupt this sequence: 1) carriers may become trapped before recombining; 2) carriers may escape from the oxide before recombining. In the latter event the oxide can become charged if one type of carrier escapes more readily than the other, leaving a net charge in the oxide. In the former case a significant charge separation can occur if trapping rates are appreciably different for the two types of carriers. Such a charge separation is expected to be intensified by the presence of an externally applied electric field during irradiation.

Both these interrupting events apparently occur in thermal oxide on silicon--some electrons created by the ionizing radiation escape from the oxide; most holes do not and are trapped, leaving the oxide with a net positive charge after the irradiating event. The holes are trapped semipermanently; the positive charge in the oxide remains for months at room temperature. It can be annealed out, however, at 300-400°C in times on the order of 1 hour.

The magnitude of the trapped positive charge varies with electric field as shown in Fig. 1. These data are based on measurements made on MOS structures. The abscissa is potential applied to the metal electrode; the ordinate is flat band voltage shift after irradiation to saturation.* With positive potential on the metal electrode the hole trapping occurs primarily in the vicinity of the oxide-silicon interface. The electrons escape the oxide through the metal electrode circuit with very little trapping. As the potential of the metal electrode is made more positive, the net effective charge trapped increases, building up adjacent to the oxide-silicon interface. Once all the traps immediately adjacent to that interface are occupied, further increase in the positive bias during irradiation widens the region of occupied traps.

With a negative bias on the metal electrode the field drifts the carriers in the opposite direction. Some electrons escape the oxide as before but they exit now via the oxide-silicon interface; the holes are trapped but are now located adjacent to the metal-oxide interface. At small negative external bias the flat band voltage shift is reduced during irradiation. As the bias increases, however, the magnitude of the effective charge induced also increases. This fact may reflect the existence of a small residual electric field in the oxide which must be compensated by a small negative bias on the metal electrode before the applied electric field dominates the carrier drift. In any event the

---

* no further shift in flat band occurs under prolonged irradiation.

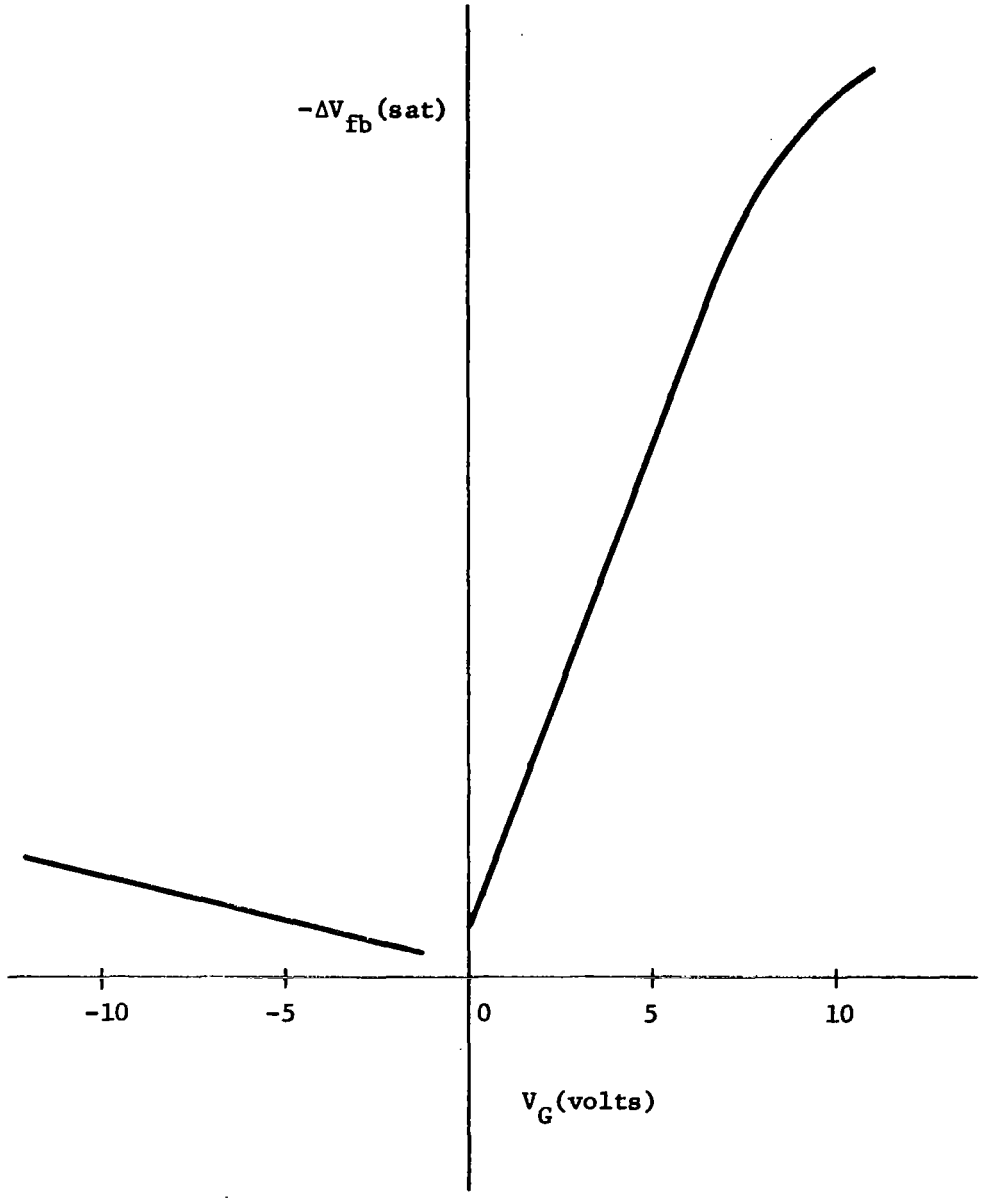

Figure 1. Voltage shift at saturation (ΔV_{fb}(sat)) as a function of gate voltage V_G during irradiation (Refs. 11,12).

space charge trapped in the oxide is higher at high field--regardless of direction--and is positive in sign.

The second influence of ionizing radiation upon oxidized silicon devices is the creation of fast interface states. These states are typically within the forbidden energy gap of the silicon and physically are located at the oxide-silicon interface. Their behavior is similar to that of other allowed electronic energy levels in that carriers can occupy and vacate these energy levels depending upon the position of the Fermi level. The presence of high densities of interface states is almost always deleterious to device operation since the effect of these states is to capture carriers that are participating in the desired device operation. These effects manifest themselves as a reduction in the beta of a bipolar transistor and in the transconductance of an MOS transistor and as a bias dependent extraneous change component in MOS capacitors. Radiation-induced fast interface states can also be thermally annealed by a temperature-time cycle similar to that used to anneal the effects of the radiation-induced space charge buildup.

Solutions Proposed and Investigated

The model of space charge buildup described in the preceding section suggests several methods of reducing oxide sensitivity to ionizing radiation:

1. Keep the electric field across the oxide at the optimum value during irradiation--the minimum point in the curve of Fig. 1.
2. Reduce the concentration of hole traps in the oxide--present evidence suggests their concentration is on the order of 10^{18} cm^{-3} (Ref. 13).
3. Alternatively increase the electron trap or recombination center concentration so that fewer electrons escape during irradiation--measurements suggest that the concentration of electron traps in thermal oxide is on the order of 10^{14} cm^{-3}, a full 4 orders of magnitude less than the hole trap density (Ref. 14).
4. Impede electron escape by creating barriers in the oxide.
5. Substitute a more radiation resistant insulator for the oxide.

Solution 1 is obvious but often impractical in operating systems and will not be considered further. Solution 2, the elimination of hole traps in the oxide, is easier said than done. Most wide-gap materials have many impurity or defect-associated levels throughout their forbidden gaps. These levels dominate the electrical properties and may be extremely difficult to eliminate in spite of the evidence that suggests a relatively low density of electron traps. A second objection to this solution is that even if the hole trap concentration could be dramatically reduced the holes still might not escape across the oxide-silicon interface as

readily as the electrons because of an interfacial barrier to hole flow. This postulation is pictured in Fig. 2 and assumes that the work function of the SiO_2 is greater than that of the silicon. Such a representation is hypothetical; the position of the Fermi level in the oxide is not known for thermal oxide; even the appropriateness of using the band model for predicting oxide electrical properties is questionable.

Investigations reported to date which have been directed toward solving the radiation sensitivity problem by reducing hole traps have been partially successful. What has been shown is that various annealing cycles and heat treatment can alter the defect structure of a given oxide which in turn does produce measurable changes in the radiation sensitivity of the oxide. The magnitude of these improvements has generally been small and difficult to separate from other variables that also influence the radiation sensitivity. Independent evidence to show that the hole trap density has actually been reduced is generally not given so these annealing cycles may well be reducing the radiation sensitivity by some mode other than that of the supposed hole trap reduction.

Solution 3, the increase of electron trap density, appears more realistic. In general increasing trapping levels or recombination centers by the addition of impurities or defects or both is easily visualized. This technique is similar to the gold doping technique used to reduce carrier lifetime in silicon switching devices. Many insulators already exhibit high trapping or recombination center densities; intuitively it would

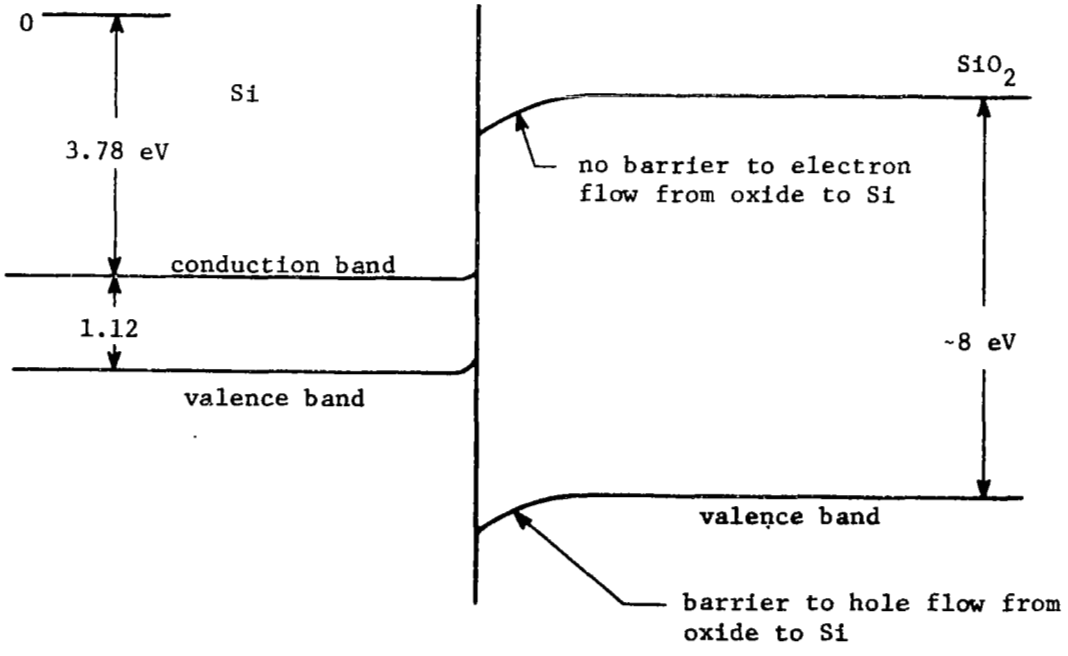

Figure 2. Band representation of oxide-silicon interface when the work function of the oxide is greater than that of the silicon.

appear possible to, in a sense, degrade SiO_2 to a similar low lifetime condition. SiO_2 exhibits a high mobility-lifetime product for electrons. For many purposes this property could be a distinct advantage but for radiation hardening it is a liability since it leads to large charge separation effects.

Among the methods that have been investigated for bringing about this type of modification are various oxide doping schemes (Ref. 15). The work of Reference 15 has included incorporation of aluminum and chromium into the thermally grown oxide in an effort to introduce defects which act as either traps or recombination centers. In general improvements were observed with all of these doping steps but the conclusion is that the annealing and heat treatments in hydrogen or helium are probably even more effective. The most radiation resistant thermally grown silicon oxide film was prepared by oxidizing silicon in an RF heated silicon system in water vapor which was followed by an in situ hydrogen treatment at 500°.

Other modifications that have been investigated include implantation of aluminum ions into the thermally grown silicon dioxide and the implantation of N_2^+ ions into thermally grown oxides. The former investigation has been performed at Hughes Aircraft (Ref. 16). The aluminum implantation appears from this brief investigation to offer no advantage over the unimplanted oxide. The interaction between high fluence N_2^+ beams and thermal oxide on silicon has been very effective and is the major task to be discussed in this contract report.

Solution 4, the insertion of potential barriers in the oxide that oppose electron flow, also seems feasible. In this scheme the oxide is coated with a second insulator so that electron flow in one direction is impeded (Fig. 3). In addition the lifetime of carriers in the added insulator may be small enough that very few electrons escape from the dielectric sandwich. These electrons become trapped (or recombine) in the insulator and partially balance the trapped holes.

One objection to this approach is that the barrier is effective against electron motion in only one direction. When the applied electric field drifts the electrons toward the silicon in Fig. 3, the electron barrier in the insulator is ineffective. It will not impede electron transport and very few electrons will become trapped in it. This restriction is inconsequential for applications in which the gate is always biased positively. The presence of an electron barrier in the oxide will reduce the radiation sensitivity of an oxide biased so as to drift electrons away from the silicon, assuming present concepts of radiation interactions are valid. For negative gate bias the electron barrier will result in a positive space charge on the oxide side of the oxide-insulator interface. If the oxide thickness in the combination oxide-insulator dielectric is less than it normally would be in an all oxide dielectric layer, it is likely that the radiation sensitivity of the

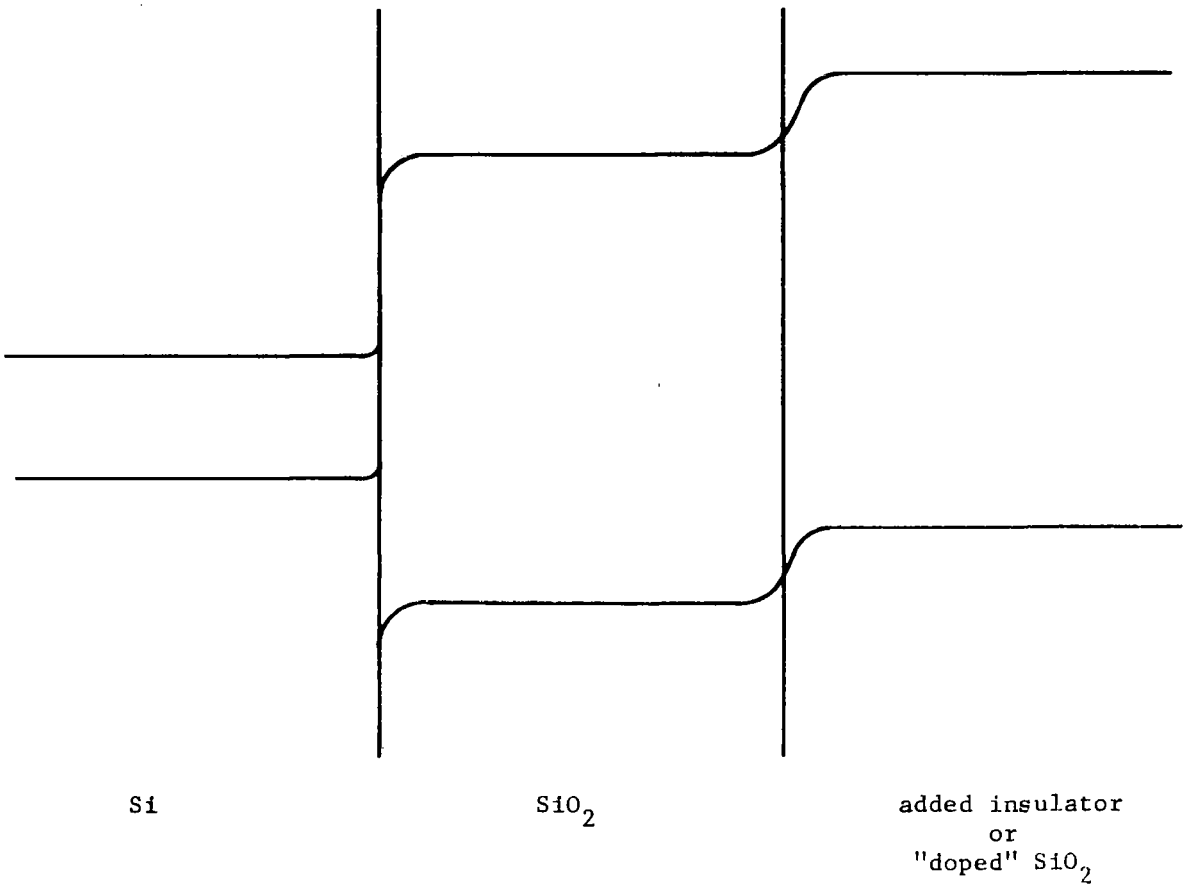

Figure 3. Electron barrier in a two-layered insulator.

combination dielectric is greater under negative bias because the positive space charge is now closer to the oxide-silicon interface than it would otherwise be.

Solution 5: The existence of many insulators already possessing the desired high concentration of electron traps--or at any rate reduced sensitivity to radiation (for example Mylar, silicon monoxide, silicon nitride) might suggest that a very practical solution is to replace SiO_2 with one of these less radiation-sensitive insulators. This solution has not been successful in the past because devices so fabricated exhibit instabilities not normally displayed by thermally oxidized silicon devices. The interface between thermal oxide and silicon is located within the

original silicon crystal and is probably a smooth but sharp transition region. Such an interface constitutes the least disruptive termination to the silicon lattice that has yet been found. Interface state densities on the order of 10^{10} cm^{-2}--far below those associated with vacuum cleaved surfaces or ion bombarded surfaces--are not uncommon.

When the interface between an insulator and silicon is formed by a deposition process, the resulting insulator-silicon systems have been found to be unstable. This instability is manifest in a shift in the capacitance versus voltage (C-V) curves under both positive and negative gate voltage and has been observed with both Si_3N_4 and evaporated SiO layers. Rapid measurements of the C-V curves indicate a parallel shift of the C-V curves under bias. The instability is similar to that observed on SiO_2 layers which have large mobile ion densities within the oxide. However, the shifts in the C-V curves are in the opposite direction to that caused by ion motion within the insulator. The simplest explanation of these instabilities is that they are due to charge injection from the silicon into the insulator over the interfacial barrier between the silicon and insulator and the subsequent trapping of these carriers in the insulator. Evidence exists for both electron and hole injection across a silicon-silicon nitride interface.

Evidence has now been reported that substitution of an entirely different material as the insulator to be used with silicon technology might be possible using Al_2O_3 as the dielectric (Ref. 17). The ability to do this could alter the operation of the silicon industry in a major fashion. For the past ten years the silicon planar technology has had thermally grown silicon oxide as the major and indeed only satisfactory insulator in the processing sequence. Thermally grown silicon oxide gives surface protection and passivation; it serves as a useful diffusion mask during oxidation; it is used as an insulating material between deposited intraconnects and the underlying silicon region; it is used as the insulator in MOS capacitors and MOS transistors and most recently has been employed as an insulator between multilayered intraconnection patterns deposited on a single substrate. In spite of considerable research, no one other material has been able to perform so many functions so well. Indeed in the past the contest has not even been close. Recent results at RCA (Ref. 17), however, indicate that Al_2O_3 may offer serious competition. Although the entire processing sequence utilizing aluminum oxide is not nearly so well developed as that of silicon oxide, early results have shown that the radiation resistance of this material is far superior to that of thermally grown silicon oxide. At the same time aluminum oxides does not exhibit the unstable interface that characterizes silicon nitride--silicon or evaporated silicon oxide-silicon interfaces. The band gap of aluminum oxide is similar to that of thermally grown silicon oxide and hence is expected to be as stable interfacially with silicon as thermally grown silicon oxide. Indeed this seems to have been borne out by data reported to date. Problems still exist in the Al_2O_3 technology

(the best films have been prepared by the plasma anodization of aluminum) but it is a very new technology as yet.

Approaches Followed by This Contract

Two approaches to radiation hardening of oxides on silicon were followed independently during this contract:

1. Modification of thermally grown oxides on silicon via ion implantation;
2. The development of evaporated silicon monoxide layers to exhibit the interfacial stability of thermal oxide.

The first technique recommended itself as a method of controllably introducing defects into thermal oxide. The ion beam introduces displacement damage and impurities, both of which should be effective in creating defect levels in the forbidden gap of the oxide. The control over both the concentration and the distribution of these defects that ion implantation makes possible cannot easily be matched by any other known technique. Such control appears necessary if one hopes to modify the bulk oxide properties without degrading the oxide-silicon interface.

The second technique is based on utilizing the known radiation insensitivity of evaporated silicon oxide by modifying the interface between the silicon and the evaporated oxide. The radiation insensitivity of bulk evaporated oxides is well documented (Ref. 18; Ref. 8) but such oxides have not been of much practical value because of the charge injection that takes place across the oxide-silicon interface. Such charge injection is consistent with a lowered potential barrier at the oxide-silicon interface for evaporated silicon monoxide (relative to that of thermally grown silicon oxide). The aim of this task was to develop methods for increasing the interfacial barrier height between evaporated oxide and a silicon substrate but at the same time preserving the radiation hard properties of the oxide.

These two approaches complement each other. In simplified terms the problem is that the oxide must possess two properties: 1) radiation insensitivity and 2) interfacial stability with silicon. Thermal oxides possess property 2 but not property 1; evaporated oxides possess property 1 but not property 2. The two tasks proposed in this contract are to find methods whereby thermal oxides could be modified to exhibit property 1 without losing advantages they already possess in regards to property 2 and conversely to modify the methods of evaporating silicon monoxide so that they can also exhibit property 2 without sacrificing the already demonstrated advantages of property 1.

The first technique has been by far the more rewarding, as might be expected from the observation that here one is simply trying to selectively degrade the oxide. Thermally grown silicon oxide is radiation sensitive because of its high electronic mobility-lifetime product. If

some modification can reduce this electron lifetime, the material should be much less radiation sensitive. Task 2, the upgrading of a deficient property, sounds more difficult and proved to be so in the course of this work. While methods for accomplishing this desired interfacial stability no doubt were identified in principle, unanticipated contamination prevented any real evaluation. Virtually all the evaporated oxides examined showed intolerable ionic contamination which precluded their evaluation as radiation hardened insulators. The charge injection type of instability was observed only on the pure evaporated silicon oxide but even here under prolonged bias-temperature stress the impurity effects eventually dominated the observations.

The ion implantation technique on the other hand operated well in its desired role. Optimum parameters for the process are not identified as yet, but qualitatively the process has been shown capable of producing less radiation-sensitive thermal oxides. Details of the work carried out in demonstrating this conclusion constitute the bulk of this report.

EXPERIMENTAL TECHNIQUES

This section describes the sample preparation used for both the ion-implanted oxides and the evaporated oxides. Methods of analysis, electron gun irradiations, Cobalt 60 irradiations and the C-V analysis were used jointly by both tasks. These techniques are described in the following paragraphs.

Sample Description and Preparation

All silicon samples used in these investigations were supplied by the Monsanto Corporation and came from the same silicon ingot. The silicon was delivered in wafer form to the following specifications:

Resistivity: 10-15 ohm-cm p-type

Dopant: boron

Orientation: (100)

Thickness: 10-15 mils

Surface Finish: 1 side polished, the other side as sawed

Oxide Thickness: 6000-8000 Å.

The as-received wafers were oxidized by the Monsanto Company to a thickness of 6800 Å. This oxide served as a protective layer throughout shipping and storage of the wafers. Prior to use this oxide was stripped in concentrated HF immediately prior to either inserting the wafer in the vacuum system for an evaporated oxide or into the oxidation furnace for a thermally grown oxide.

The thickness of dielectric utilized throughout the experiments was 2000 Å. This value of thickness was maintained whether the oxide was thermally grown or evaporated. For thermally grown oxides both steam and dry oxygen were used to grow the oxides. In the case of the steam oxides the cycle consisted of a 5-5-5 cycle in which the wafer was loaded in dry oxygen for the first 5 minutes, the carrier gas was then switched to steam for the next 5 minutes and finally returned to dry oxygen for the concluding 5 minutes of the oxidation cycle. All these steps were at a furnace temperature of 1100°C. The dry oxygen cycle consisted of a 1200°C exposure to dry oxygen for 1 hour. The wafers were removed from the furnace rapidly following the oxidation cycle.

Following oxidation all wafers were coated with aluminum in an Ultek ion pump system, employing an electron gun heater. Evaporation was carried out through a molybdenum evaporation mask consisting of an array of 15 mil diameter holes on 20 mil centers. The thickness of the aluminum during evaporation was measured by a crystal monitor; evaporation was stopped at a thickness of 1000 Å.

Most units irradiated throughout the contract period were then exposed to a hydrogen annealing cycle at 400°C for 1 hour. Early units examined did not always receive this treatment but subsequent evaluation of annealed versus unannealed units showed that there was more reproducibility among the hydrogen annealed units in that the presence of interface states (as indicated by the slope of a C-V measurement, see following section entitled "Capacitance-Voltage Analysis") was minimized by including this step. The improvement manifested itself not only in the initial properties of the capacitor but particularly in the properties of the capacitor following various irradiations.

The units were then scribed and diced so as to fit on 12-pin TO-5 headers. Each chip was scrubbed by hand onto such headers and the outermost 15 mil aluminum electrodes were contacted by a ball bonded gold wire. The wire was positioned so as to minimize the shadowing of the gold wire on the aluminum electrode. The area of the ball bond was approximately 4 mils in diameter. The temperatures of the chip during the scrub bonding was approximately 450°C; during wire attachment the chip temperature was approximately 320°C. A heated capillary was used during the ball bonding.

Capacitance-Voltage Analysis

The primary measurement made in analyzing the properties of the various oxides and modified oxides prepared during this contract was the capacitance-voltage property of a metal oxide silicon structure (MOS). This measurement has been well publicized in recent years (Refs. 19,20). While the method is extremely powerful for understanding the properties of the oxide-silicon interface, the only quantitative number recorded during these experiments was that of the flat band voltage. The flat

band voltage is the value of applied voltage on the metal electrode at which the MOS capacitor has the value of capacitance corresponding to zero potential applied to the ideal capacitor (the ideal capacitor is a capacitor in which all voltages applied to the metal electrode are balanced by charges in the silicon surface space charge region). Consequently the flat band voltage is a measure of the departure from the ideal capacitance. The assumption is that in these experiments the value of flat band voltage departs from the ideal capacitor primarily by those charges introduced during the irradiating event. The procedure is to measure the initial, pre-irradiation value of flat band voltage and to subtract this value from the value of flat band voltage following a given exposure to ionizing radiation. The increase in the magnitude of the flat band voltage is taken to be a measure of the charge introduced into the capacitor by the irradiation. As discussed in the Introduction these charges can be either in the form of an oxide space charge or as interface states at the oxide-silicon interface. The flat band value does not distinguish between these two sources of charge, although the slope of the capacitance versus voltage curve is degraded from the ideal capacitor behavior by the presence of interface states which are being charged or discharged during the voltage sweep. Only qualitative note of slope degradation was made during this experiment. Results strongly recommend that future experiments include a quantitative measure of the interface state density component such as the conductance-voltage measurements developed by Nicollian and Goetzberger (Refs. 21,22).

Typical C-V curves are shown in Fig. 4. The flat band voltage is measured in the depletion branch of the curve. The inversion branch behavior was largely ignored during these measurements.

Figure 5 shows the circuit schematic used to record these plots. Various methods of permanent record were employed throughout the year but in all cases consisted of an X-Y type record showing capacitance versus voltage.

Electron Gun Irradiation

The chief source of irradiation throughout the contract was a Brad-Thompson electron gun similar to that reported in NASA CR-1088 (Ref. 11), the final report of Contract NAS1-6900. Much the same technique as described there was employed here. Modifications were necessary to accommodate the samples, now mounted on TO-5 headers rather than held as whole wafers under mechanical springs.

The electron energies used varied from 4 keV to 20 keV, the latter energy being used for a large majority of the irradiations. Fluences typically varied from 10^{12} e/cm^2 up to 10^{16} - 10^{17} e/cm^2. To keep this fluence range in a convenient time scale the flux used varied throughout such a radiation cycle, starting at a level of 6×10^{10} e/cm^2-sec. The

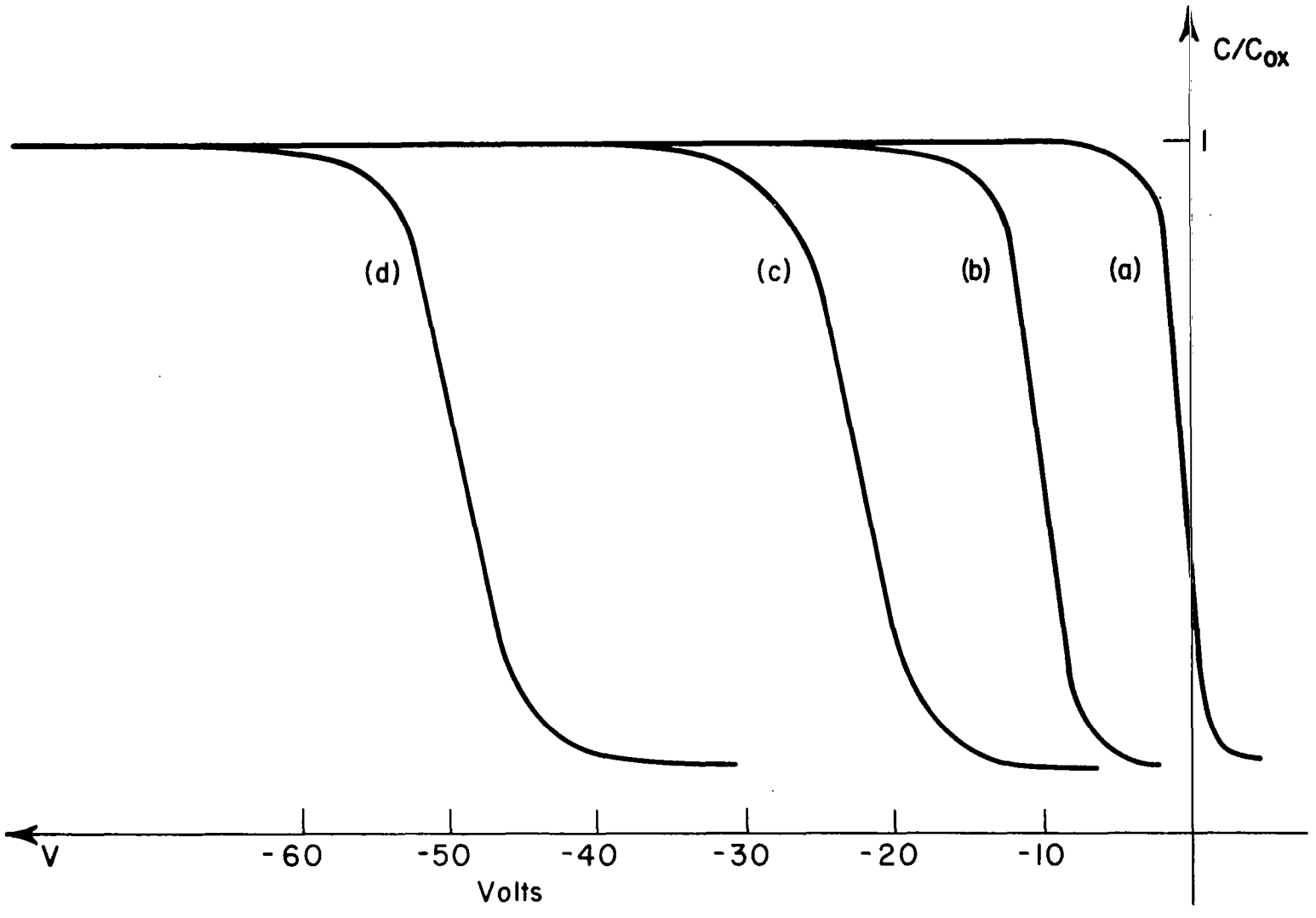

Fig. 4 TYPICAL C-V PLOTS FOR a) THERMAL OXIDE b) IMPLANTED THERMAL OXIDE c) IRRADIATED IMPLANTED THERMAL OXIDE d) IRRADIATED THERMAL OXIDE (Co 60 IRRADIATIONS AT + 8 V GATE BIAS AND 1.7×10^7 RADS.

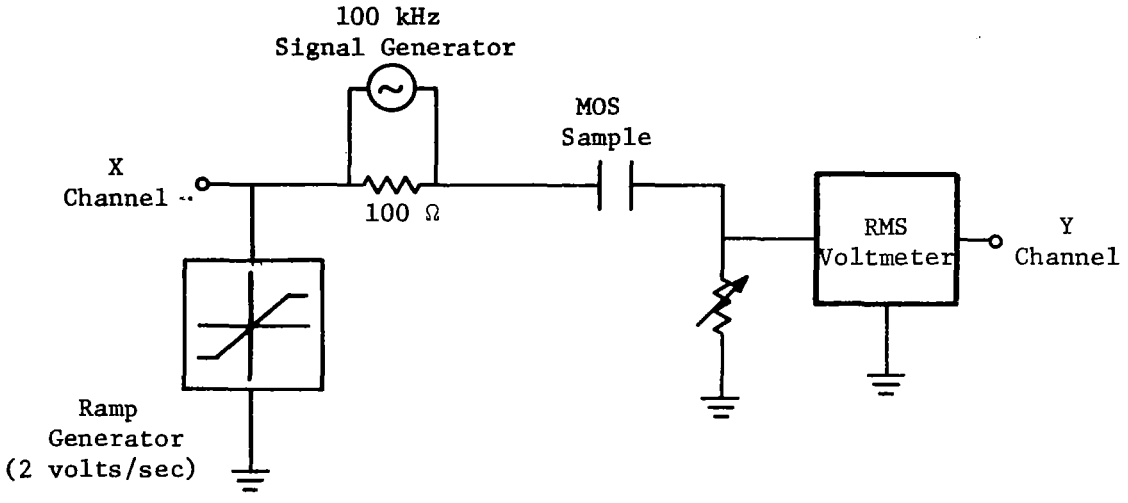

Figure 5. Schematic of C-V measuring apparatus.

highest flux used was 6×10^{14} e/cm^2-sec. At 20 keV this electron fluence range corresponds to approximately 5×10^5 rads to 5×10^9 - 5 10^{10} rads.

The technique employed permitted the same silicon chip which contained 8, 10 or even more identical capacitors to be biased at different values during irradiation. Customarily the technique employed consisted of biasing 2 units at +8 volts, 2 units at +4 volts, 2 at zero, 2 at -4 and 2 at -8. The uniformity of the electron beam was judged adequate to assume that no significant variation in flux occurred over the surface of the chip. Among the initial experiments performed to verify this assumption was irradiation of several chips with all units biased identically and comparing the charge buildup of each unit. Typically these units varied less than 5% from each other for the same bias with the exception of the initial dry oxygen oxide investigated. For this reason dry oxygen oxides were not used in the early stages of the program and all early data were taken on steam grown oxides.

Cobalt 60 Irradiation

An alternative source of ionizing radiation used during the experiments was the Co-60 source available at RTI. This source emits approximately

0.25 megarads per hour at a distance of 6 centimeters from the center of the source housing. By mounting headers on the inside of a cylindrical container, the source could irradiate as many as 12 headers simultaneously. The various units on the different headers could be biased at the desired voltages throughout the irradiation, much the same as the units were biased for exposure to radiation from the electron gun.

During exposure to the CO-60 source a dry nitrogen flow continually swept by the samples which were housed in the cylindrical containers surrounded by a polyethylene bag. Failure to control the atmosphere during irradiation initially resulted in a large incidence of short or burnt-out capacitors.

The chief advantage of the Co-60 source is that it is a commonly used source of gamma rays, and allows ready comparison between the results measured on our samples and those published by others. The biggest disadvantage for this work was the relatively low flux available so that in a practical sense the maximum fluence obtainable was on the order of $1 - 4 \times 10^7$ rads. The electron gun, on the other hand, permitted 10^8 or 10^9 rads or more to be reached in relatively short times and hence the gun was the preferred irradiation tool.

ION IMPLANTATION

As described in a preceding section, ion implantation constituted one of the techniques used to improve the radiation sensitivity of thermal oxide on silicon. In this technique one starts with a standard thermally grown oxide and attempts to modify the properties of this oxide so as to preserve the interfacial stability that is normally shown by interfaces between silicon and thermally grown oxides but at the same time reduce the sensitivity to ionizing radiation that is also normally shown by thermally grown oxides. Several methods are possible. One is to introduce the impurities into the oxide since impurities perturb the electronic levels of a material and alter carrier kinetics. Ion implantation is capable of introducing carefully controlled concentrations of impurities, as is well appreciated in silicon technology. A second technique for reducing radiation sensitivity would be to introduce structural imperfections. Ion implantation also does this. Consequently ion implantation seems to be a reasonable method to follow in modifying the properties of a thermally grown oxide particularly when one considers that the depths of penetration and the density of the implanted beam can be carefully controlled by the independent variables of the implantation process. This section describes briefly the theory of implantation, the apparatus used to carry it out and the resulting measurements made on the implanted samples.

Background and Theory of Ion Implantation

Ion bombardment has been studied over the past hundred years primarily by nuclear physicists interested in studying the interactions between an incident high energy, charged particle and a target. This type of interaction led to the famous Rutherford scattering model in which the interaction between alpha particles and the atoms of a target crystal was shown to be largely electrostatic in nature; that is, the incident charged particle was shown to be scattered by the electrical field associated with an atom, not requiring a direct collision with the nucleus.

Over recent years ion bombardment has been used as a technique for cleaning surfaces, since one consequence of a high energy bombardment is to knock off surface atoms from the target. This technique is particularly effective when the surface is covered with a weakly adhering foreign layer. Suitable control of the energy and mass of the bombarding particle can serve to eliminate the surface adsorbate without greatly disrupting the target surface proper. Under higher bombarding energies surface layers of the host target lattice can also be dislodged, as in sputtering.

In the past 10-15 years, appreciation of the possibility of trapping the bombarding ions in the host lattice has been recognized and to some extent capitalized upon. It is only over the most recent five or six years, however, that the technique of doping silicon by ion implantation has become practical. By employing suitable dopants in silicon, such as boron, phosphorus and others, and utilizing appropriate annealing cycles which permit the trapped implanted ions to become incorporated substitutionally into the host silicon lattice, useful devices have been prepared and are now commercially available. The types of devices that have been successfully fabricated include solar cells, field effect transistors and other single junction devices. Bipolar transistor fabrication has not yet been demonstrated to be a practical technique, presumably because of the inevitable lifetime degradation that accompanies the displacement damage introduced during the implantation process itself.

In the use investigated during this contract displacement damage was viewed as a desirable interaction, provided, of course, it could be controlled and localized in that region of the oxide in which it was desired. Chemical effects could also be beneficial but generally do not predominate in an implantation experiment unless suitable annealing steps are taken. The usual technique for avoiding the undesirable effects of displacement damage during implantation into silicon include carrying out the implantation process itself at a temperature in the vicinity of 600°C or subjecting the implanted silicon to a post-implantation annealing cycle of at least 600°C. This temperature permits the damage to the silicon lattice to anneal essentially as fast as it occurs or, in the post-implantation anneal, to restore the broken bonds. The problems encountered with the bipolar transistor fabrication suggests that this annealing is not 100% effective--some residual degradation in lifetime persists after the implantation--but the concentration of active impurities introduced can be

made to approach closely those that the implantation parameters predict. This last observation simply reflects the fact that most of the introduced impurity ions can be seen to be contributing to the doping of the semiconductor as based on measurements of resistivity and Hall coefficient following implantation.

In the implantations performed during this contract, the oxidized silicon wafer was not heated above room temperature during any of the implantations. Each wafer was mounted on a large metal wheel which served as a heat sink to minimize any temperature rise that the ion beam itself might tend to introduce. While no specific temperature measurement was made of either the wafer or the wheel on which it was mounted during the implantation, the conditions of the experiment suggest that the wafer temperature did not exceed room temperature by more than 10-15°C at any time. Certain of the implantations were actually carried out with a cold finger jutting into the vacuum chamber in which they were mounted, although the purpose of the cold finger was not temperature control but that of an aid to vacuum pumping.

Two important parameters of any implantation are range and concentration of the implanted particles. These values are controlled primarily by the fluence of the bombarding particles and the energy to which they are accelerated prior to implantation. The distribution of the particles in the target depends upon the structure of the target in the case of crystal materials; for the implantations carried out here the target is the amorphous silicon oxide, thermally grown on silicon. The assumption of an amorphous target simplifies the calculation of ranges in that the collisions between the bombarding ions and the target atoms can be assumed to be random. Under this assumption each bombarding particle undergoes a series of scattering collisions with the atoms of the target, losing some energy at each such collision until finally it is in thermal equilibrium with the target atoms.

The range problem then becomes that of solving a series of isolated, classical two body collision problems. Various assumptions as to the nature of the interaction between the two interacting particles are possible:

(1) A Coulomb potential ($V(r) = K\frac{q^2}{r}$). This type of interaction potential was assumed by Rutherford in his classical treatment of the scattering of alpha particles.

(2) The hard sphere potential ($V(r) = 0$ for $r >$ 2 particle radius; $V(r) = \infty$ for $r <$ 2 particle radius).

(3) A screened Coulomb potential such as the Thomas-Fermi interaction potential. The Thomas-Fermi interaction potential is of the form $V(r) = \frac{Ke^2}{r} f\left(\frac{r}{a}\right)$. The factor $f\left(\frac{r}{a}\right)$ is added to the Coulomb

potential to account for the screening of the nuclear charge by the electrons surrounding an atom or ion. The Thomas-Fermi interaction function is of the form $f(\frac{r}{a}) = \left\{ \frac{\frac{r}{a}}{[(\frac{r}{a})^2 + C^2]^{1/2}} \right\}$

where r is the distance between the two interacting particles; a, a screening parameter, equals $0.885\ a_0(Z_1^{2/3} + Z_2^{2/3})^{-1/2}$; a_0 is the Bohr radius, the radius of the first Bohr orbit of an electron in the hydrogen atom; Z_1 is the atomic number of the bombarding atom; Z_2 is the atomic number of the target atom; C is an adjustable parameter.

Based on the Thomas-Fermi screening function as listed above, Lindhard, et al., (Ref. 23) have developed expressions for the range of bombarding ions in various targets. The problem is presented in terms of various ranges such as shown in Fig. 6. The range of greatest practical interest

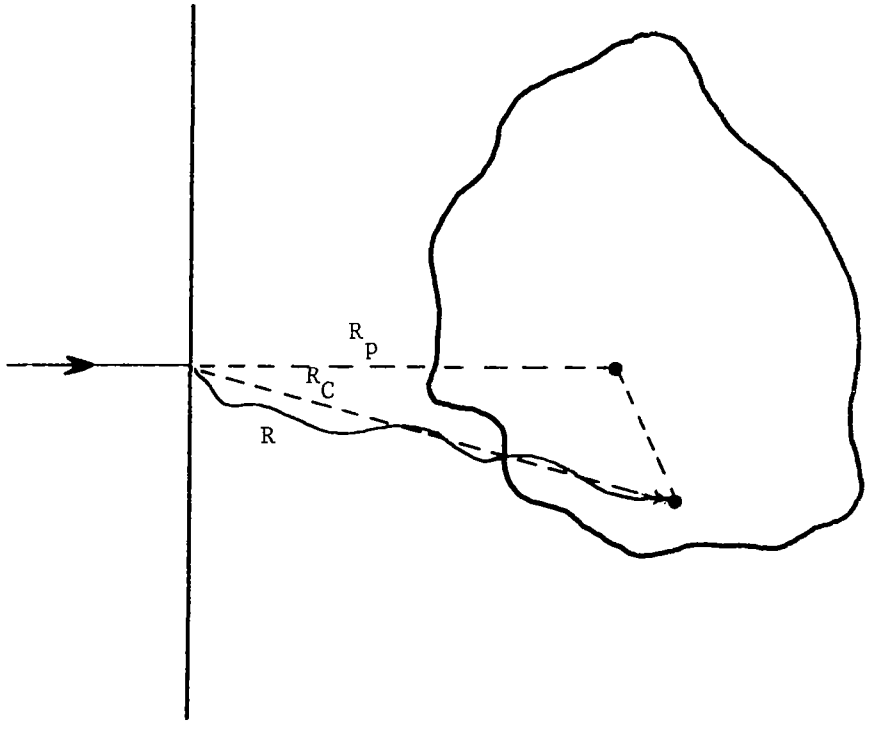

Figure 6. Ranges associated with ion implantation (Ref. 23).

(in the sense that it is a measurable range) is the range labeled R_p. This gives the depth of an implanted particle below the surface of the target in the direction of the implanted beam. In Lindhard's treatment of implantation into an amorphous target the collision problem is viewed as a series of random collisions resulting in a Gaussian distribution of values of R_p about a mean value, $\bar{R}_p$. Using these expressions, Gibbons (Ref. 24) has computed values of projected range (R_p) and the standard deviation of projected range (ΔR_p) for various ions implanted into silicon. In the work performed here, Gibbons' computer calculations were used to estimate the range and concentration, even though the target material utilized in his calculations was silicon and the implantations investigated here were in silicon dioxide. These target materials are not very different in terms of density (density of silicon is 2.3 grams/cc; silicon dioxide, 2.2 grams/cc) and average atomic number (the atomic number of silicon is 14; the average atomic number of silicon dioxide is 10).

One further assumption was made in using these tables--the disintegration of the accelerated nitrogen molecule, N_2^+, into a nitrogen atom and ion; $N_2^+ \rightarrow N_1^+ + N_1$. This reaction assumes that the nitrogen molecule breaks into an atom and a N_1^+ ion immediately upon striking the silicon dioxide surface or before (but after being accelerated and analyzed, see Fig. 7). All range data then were calculated on the basis of two 25 keV nitrogen particles striking the silicon dioxide surface perpendicularly. For a 25 keV nitrogen particle, the assumed values of R_p and ΔR_p are 617 Å and 222 Å respectively. The relation between concentration and fluence adopted from Gibbons (Ref. 24) is: $\hat{N}(cm^{-3}) = 0.8\ N_2^+\ (cm^{-2})$. $\hat{N}$ is the peak concentration of the implanted species which occurs at a depth of R_p; $N_2^+\ (cm^{-2})$ is the implantation fluence. The concentration is normally distributed about $\hat{N}$, decreasing one decade at distances of $R_p \pm 2\Delta R_p$ and by two decades at $R_p \pm 3\Delta R_p$, etc.

The N_1^+ ion is neutralized by electron capture at some point along its path and comes to rest as an N_1 atom so no attempt was made to distinguish between the range of the N_1 atom and the N_1^+ ion. The differences in the range of these two particles is assumed to be negligible, although the scattering problem is modified by the presence of additional electrons on the N_1 atoms.

Apparatus for Ion Implantation

The apparatus used to carry out the implantations of this contract is pictured schematically in Fig. 7. This apparatus is a 400 keV van de Graff accelerator built by High Voltage Engineering Corporation

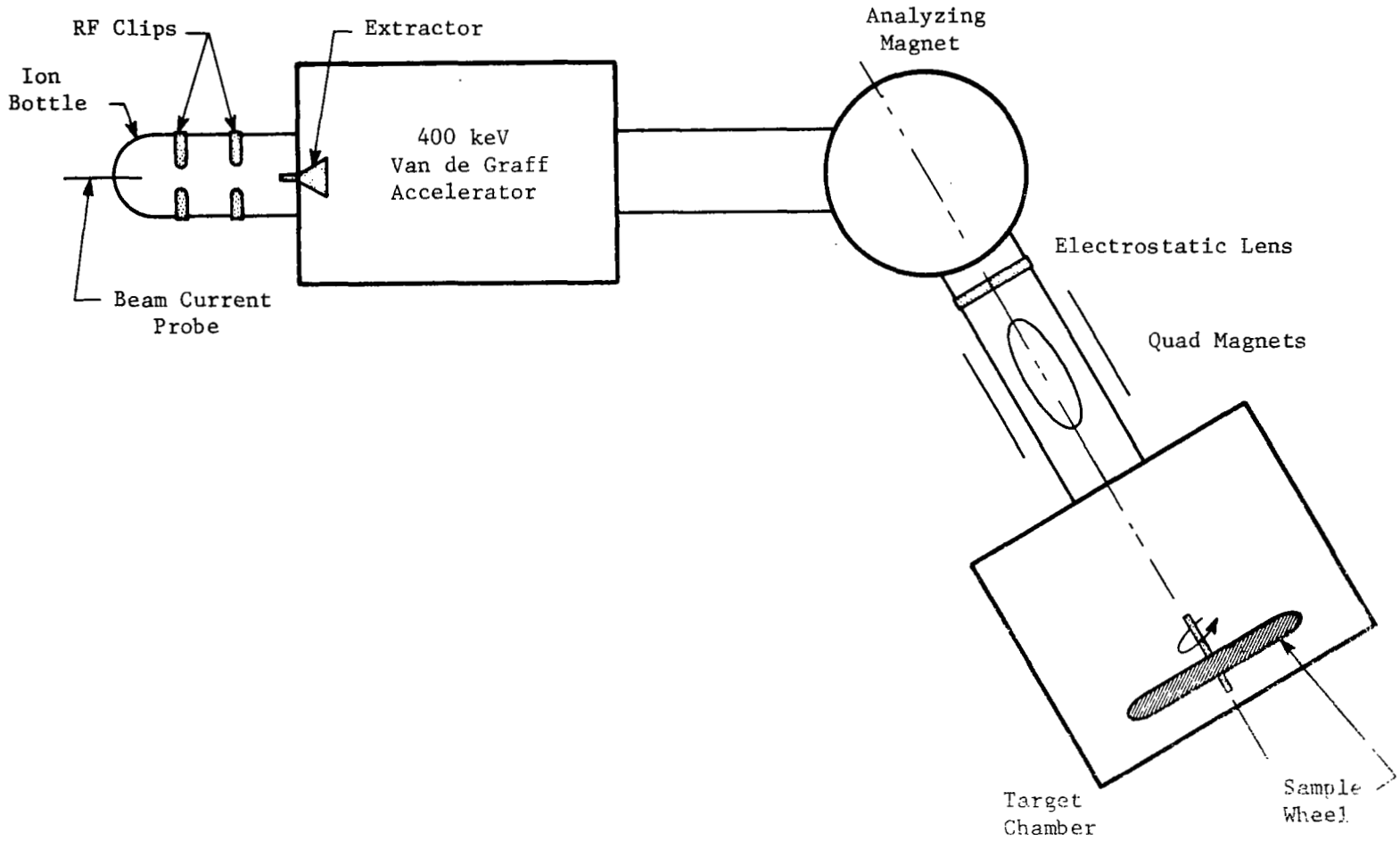

Figure 7. Ion implantation apparatus.

and housed at the Materials Radiation Laboratory of the Chemistry and Physics Branch of AMPD, Langley Research Center. The unit utilizes an RF ion source. The gas to be ionized and implanted is bled into a glass envelope which is capacitively coupled to a 90 watt RF oscillator. The oscillator is tuned for maximum energy transfer, creating a large number of ions in the gas. These ions are generally singly charged positive and are extracted from the plasma within the envelope into an accelerating field. The accelerator in this installation is of the van de Graff type in which the high accelerating field is spread out over 2 or 3 feet by a number of spacers insulated with an appropriate gas. The ions emerging from the accelerator are directed into an analyzing magnet which is capable of isolating the ions into species of specific mass-to-charge ratios. By adjusting the magnetic field the desired species can be directed onto the target area. For the experiments performed here the beam was spread out by a quad magnet arrangement following the analyzing magnet. The purpose of the quad magnet was to obtain as uniform a beam pattern as possible.

In actuality, this beam was somewhat unstable and was sensitive to small adjustments so that for most implantations the beam uniformity was no better than $\pm$ 30% of a nominal value. Even here, the area over which $\pm$ 30% was maintained varied with the energy of the implantation and with time. The beam current was not measured directly during the implantation but was scanned at various times by a movable Faraday cup. The operating sequence was approximately: 1) the ion beam was turned on and set to the nominal values corresponding to the desired implantation. 2) the movable Faraday cup scanned the beam, measuring the current at various points within the target chamber in a left to right and up and down direction. 3) The fine adjustments were made so as to produce the most uniform scan pattern. 4) The sample wafer was inserted in front of the beam and implanted to a desired fluence level. 5) The ion beam was rescanned following the completion of the implantation process to assure that the beam had remained constant throughout.

In the case of long runs at high fluence levels the implantation process was interrupted once or twice to confirm that the ion beam had not drifted substantially. The interruption was assumed not to influence the implantation in any way.

The target chamber of the accelerator consisted of a large aluminum box which contained a wheel capable of holding 5 wafers in addition to the scanning Faraday cup. The target chamber was pumped by an oil free turbo-molecular pump and was operated at about 10^{-5} torr. Remaining lines in the ion path were also evacuated to pressures in the same vicinity by various pumps strategically located along the path. The total ion path length from the ion source to the target is on the order of 25 feet.

RESULTS

Two series of implantations were carried out during the course of the contract. The fluences, energies, species and targets during

implantation are summarized in Tables 1 and 2. All evaluations of radiation sensitivity were carried out on the 2000 Å oxides. At this thickness the only implantations which yielded useful capacitors were those carried out at an implantation energy of 50 keV. The higher implantation energies degraded the properties of the oxide so that the dc resistance was severely reduced. No electrical evaluation was made on the thicker oxides implanted at the higher energies, although measurements of IR absorption and etch rates were carried out on these wafers.

Table 1. First Implantation Series
(All N_2^+ Implantations)

Wafer No.	Energy	Fluence (cm^{-2})	Oxide Thickness* (steam)
8	50 keV	10^{15}	2000 Å etch-back
9	↓	↓	" "
10	↓	↓	2000 Å thermal
11	↓	↓	" "
12	↓	10^{16}	" "
7	↓	10^{16}	2000 Å etch-back
14	↓	10^{17} spot	2000 Å thermal
13	200 keV	10^{15}	" "
2	↓	↓	6800 Å as grown
3	↓	↓	" "
5	↓	↓	5000 Å etch-back
6	↓	↓	" "
1	↓	10^{16}	6800 Å as grown
4	↓	↓	5000 Å etch-back

* etch-back means that the final oxide thickness was reached by etching a 6800 Å oxide to the final thickness.

Table 2. Summary of Second Implantation Series

	Wafer No.	Oxide (2000 Å dry)	Implantation Parameters		
			Species	Energy	Fluence
Group I	7A	Fairchild	N_2^+	50 keV	10^{16} cm^{-2}
	8A	"	"	"	10^{15} "
	9A	"	"	"	10^{14} "
	13A	RTI	"	80 keV	10^{15} "
	14A	"	"	120 keV	10^{15} "
Group II	6A	Fairchild	O_2^+	50 keV	10^{16} "
	5A	"	"	"	10^{15} "
	10A	RTI	"	"	10^{14} "
	11A	"	"	80 keV	10^{15} "
	12A	"	"	120 keV	10^{15} "
Group III	2A	none	"	50 keV	$10^{16}+10^{18}-10^{19}$ spot
	3A	none	"	80-120 keV	"

Of the implantations performed at 50 keV the limitation in fluence was 10^{16} N_2^+ cm^{-2}. Several implantations were carried out at 10^{17} cm^{-2} and invariably resulted in degraded dielectric behavior. Fluences less than 10^{15} generally produced little or no change from the unimplanted oxide so that little data were gathered on those samples. Most of the data to be reported here were on oxides 2000 Å thick implanted with 50 keV N_2^+ particles at a fluence of 10^{16} cm^{-2}.

The most significant result was the large reduction observed in the radiation sensitivity of the implanted oxide when compared with similar thermal oxides that were not implanted. This conclusion is based on data shown in Figs. 8-12. All these plots show charge buildup brought about by exposure to various sources of irradiation. The abscissa in all plots is fluence; the ordinate, shift in flat band voltage. For the 2000 Å oxide

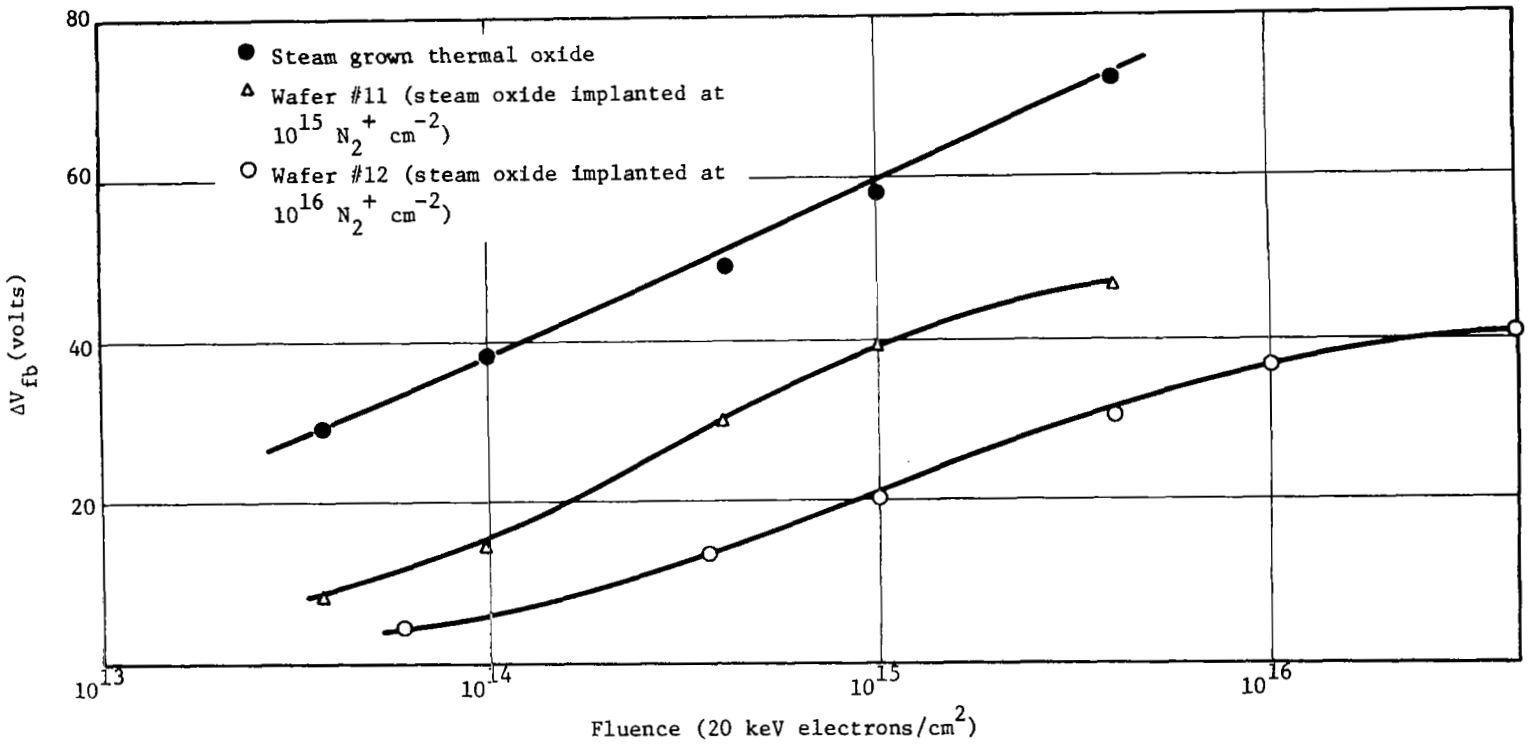

Figure 8. The influence of N_2^+-implantations upon radiation-induced charge buildup in thermal oxides. Oxide thickness: 0.2 μm; aluminum electrode thickness: 0.1 μm; silicon impurity concentration: $N_A \sim 1.6 \times 10^{16}$ cm^{-3}; bias on aluminum electrode during electron irradiation: +2 volts.

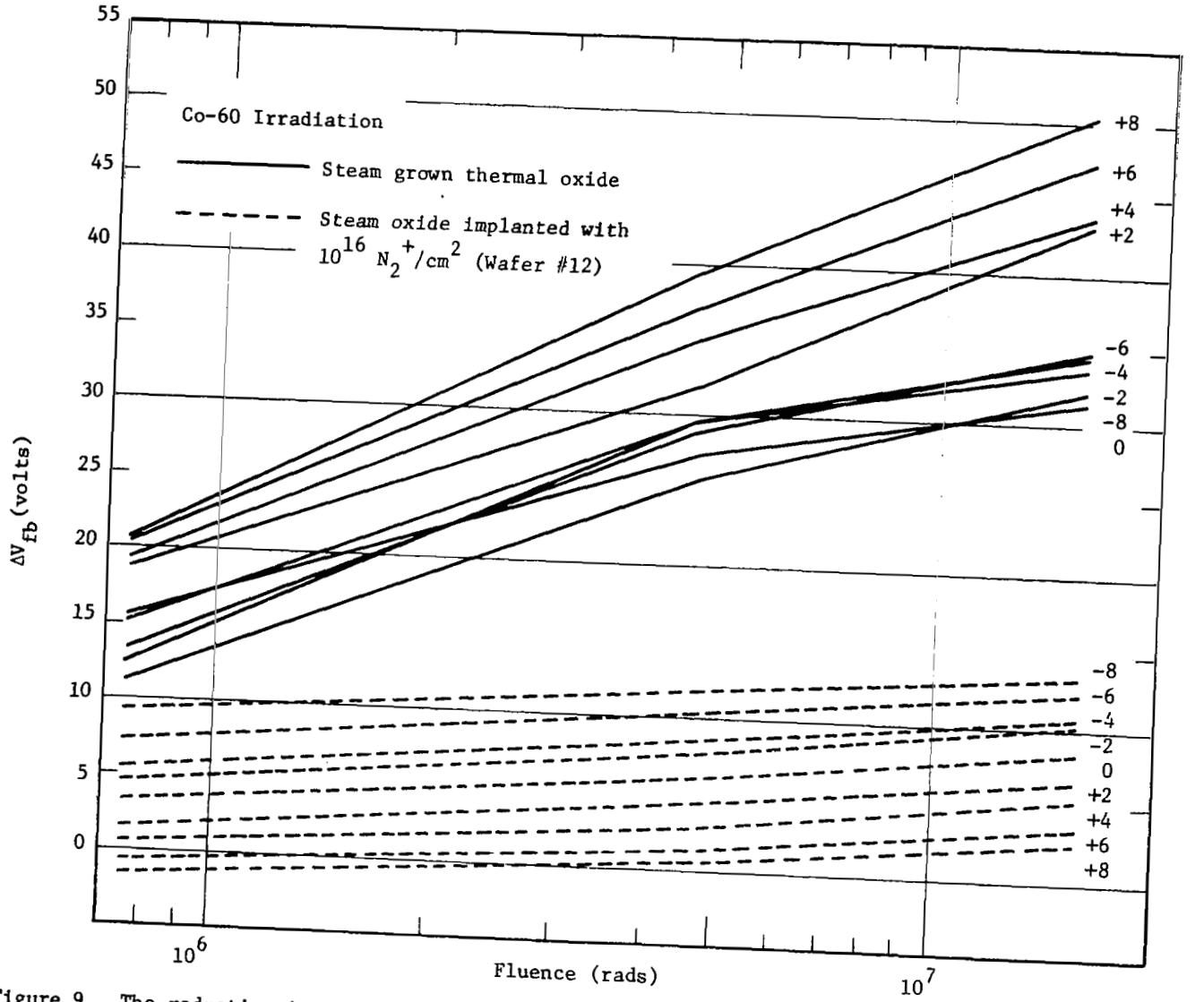

Figure 9. The reduction in radiation-induced charge buildup in thermal oxide on silicon brought about by ion implantation. ΔV_{fb} is the change in flat band voltage (ΔV_{fb} = 10 volts corresponds to 1×10^{12} surface charges/cm^2; bias during irradiation as shown).

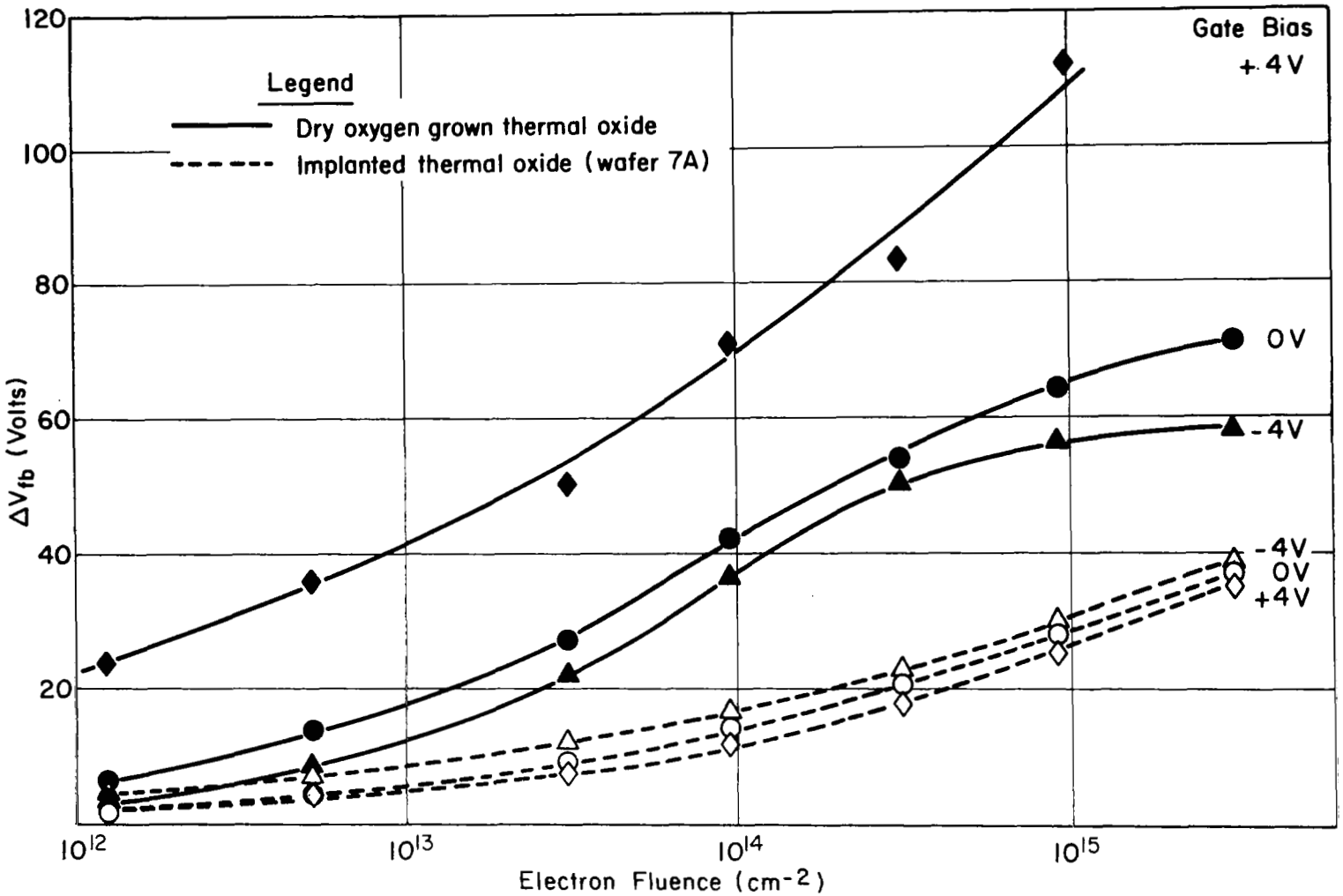

Fig. 10 COMPARISON OF CHARGE BUILD UP INDUCED IN IMPLANTED AND NON-IMPLANTED THERMAL OXIDES BY 20 KeV ELECTRON IRRADIATION

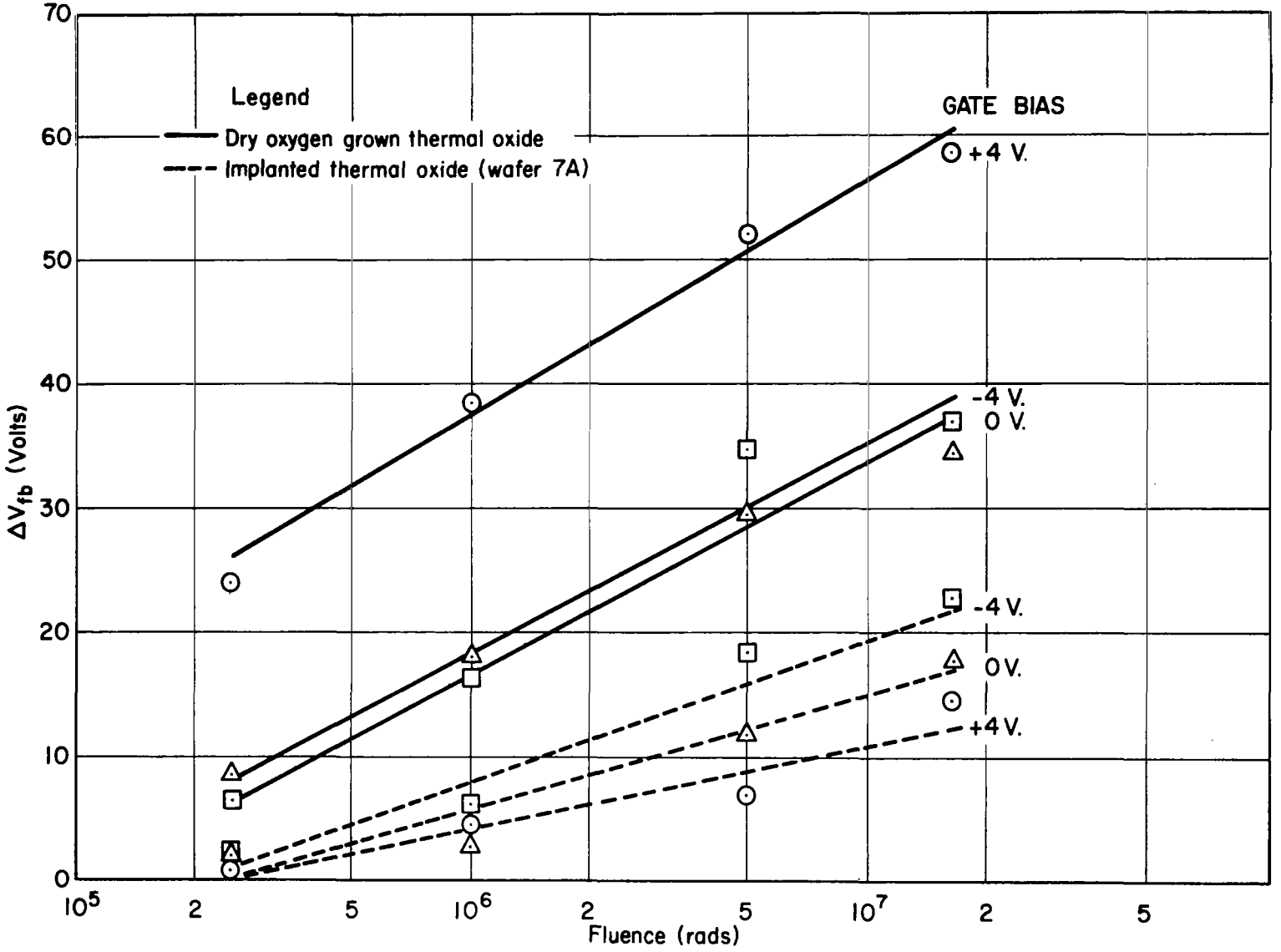

Fig. 11 COMPARISON OF CHARGE BUILD UP INDUCED IN IMPLANTED AND NON-IMPLANTED THERMAL OXIDES BY CO 60 IRRADIATION

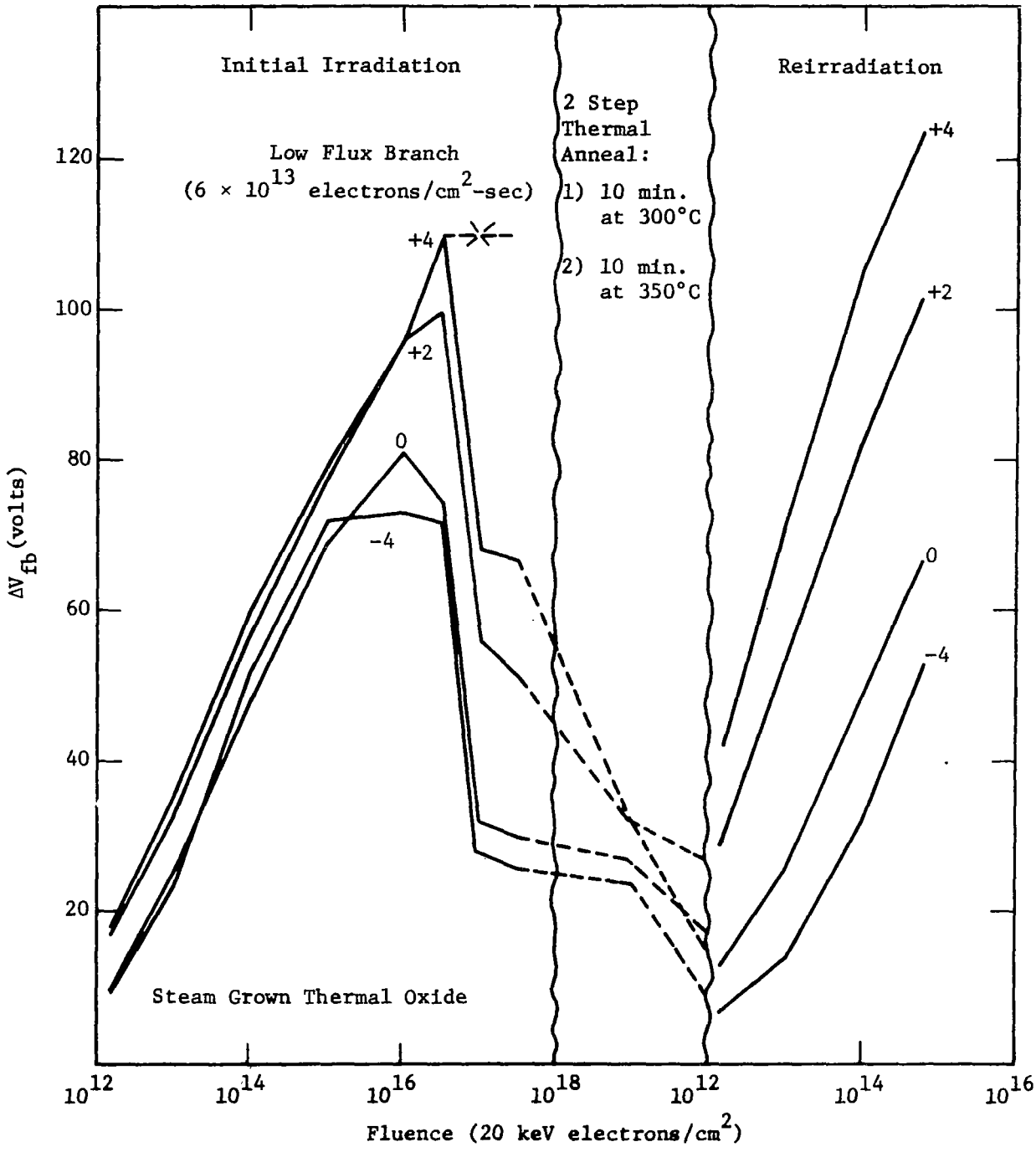

Figure 12. The dependence of charge buildup upon irradiation history and flux (bias during irradiation as shown on each curve).

used in all these measurements a shift in flat band voltage of 10 volts corresponds to a charge introduction into the oxide of approximately 1×10^{12} charges/cm^2. Figures 8 and 9 are steam grown oxides. Figure 8 is exposure to 20 keV electrons; Fig. 9, Cobalt 60. Figures 10 and 11 are data gathered from measurements on dry oxygen grown oxides. These oxides are those that were prepared for us by B. E. Deal of Fairchild R/D. As can be seen from Figs. 10 and 11 the results are substantially the same as those on the steam grown oxides.

The key point is the drastically reduced magnitude of the change in flat band voltage during irradiation under positive bias that characterizes the implanted oxide.

Another important feature of the data is the lack of bias dependence characteristic of a charge buildup for the implanted oxide. This observation has characterized all implanted wafers. In most cases the bias sensitivity is reversed in that the charge buildup is slightly greater with a negative bias on the aluminum electrode but this bias dependence is small. At all biases the charge buildup is reduced in the implanted oxides over that in the non-implanted oxides, although the magnitude of the reduction is not nearly so pronounced at a bias of, say, -4 volts as it is at a bias of +4 volts.

Typical C-V plots for both implanted and non-implanted thermal oxides, before and after positive bias irradiation, were sketched in Fig. 4. The displacement between curves "c" and "d" would be smaller with zero or negative gate biases. Flat band voltage shifts produced by implantation at 10^{16} cm^{-2}, 50 keV N_2^+ generally ranged from 7 to 15 volts. Using the Gray-Brown technique for measuring interface state density (Ref. 25), these initial shifts were found to be partly due to interface states introduced during implantation. The mean projected range of a 25 keV N_1^+ or N_1 particle is approximately 600 Å. At this depth the nitrogen concentration is on the order of 10^{21} cm^{-3}. Even at the distant interface, some 1400 Å away, however, the concentration of nitrogen could be as high as 10^{14} to 10^{15} cm^{-3}, assuming the predicted Gaussian distribution about the maximum. A reduction in the implantation energy may be desirable to reduce the nitrogen reaching the interface.

These data are generally consistent with a model which pictures the bias dependence component of radiation induced charge buildup as being caused by the creation of positive space charge in the oxide, while the bias independent component of charge buildup is attributable to interface states. The reason for the reversed bias sensitivity usually observed in implanted samples during irradiation has not been clearly established. The same phenomenon has been reported in phosphorus-glass coated oxides and in MNOS capacitors and has been attributed to a hole-electron barrier within these modified insulators (Ref. 16). Our results suggest that one

effect of nitrogen ion implantation is to introduce such a barrier within silicon dioxide.

The reduced radiation sensitivity evident in Figs. 8-11 was attributed to displacement damage initially. Two experiments were conducted to investigate this hypothesis.

The first of these experiments consisted of irradiating the oxide with high fluences of 20 keV electrons. The idea behind this experiment was that the oxide itself might undergo displacement damage induced by the electron beam. For displacement damage to occur, the relationship between the binding energy of an oxygen atom in the SiO_2 network, E_d, and the energy of the bombarding electron, E_t, is:

$$E_t \simeq 7.4 \times 10^3 E_d \ .$$

This relationship is derived from conservation of energy and momentum before and after collision. When E_t is 20 keV, $E_d \simeq 2.7$ eV. This value of E_d is not incompatible with the activation energy for oxygen diffusion in vitreous silica. Activation energies deduced from oxygen diffusion work vary between 1.3 eV and 3.1 eV (Ref. 26). The large variation in activation energy reported may reflect the structural perfection of the silica glass. Doubly-bonded oxygen (the oxygen is bound to two nearest neighbor silicon atoms) requires more energy to displace than a singly-bound oxygen atom. A very common defect in silica glass is the existence of broken oxygen-silicon bonds, resulting in large, variable concentrations of singly-bound oxygen atoms. Based on observed activation energies, displacement of oxygen atoms in SiO_2 seems possible by 20 keV electron bombardment. The silicon atoms of SiO_2 are more tightly bound, being attached to four nearest-neighbor oxygen atoms, and are not expected to be displaced by this low energy electron bombardment.

The second experiment was the implantation of O_2^+ into the oxide at substantially the same energies and fluences used in the N_2^+ experiment. Oxygen and nitrogen are similar species, mass wise, being neighbors in the periodic table, and the range data used for nitrogen should be roughly applicable for oxygen as well.

High Fluence, Low Energy Electron Irradiation

Figure 12 shows the effect of high fluence electron irradiation upon the radiation sensitivity of a steam grown thermal oxide. The striking feature of this data is the decrease observed in flat band voltage at an

electron fluence of 10^{16} to 10^{17} cm^{-2}. In particular, there is a large decrease in the flat band voltage between the points taken at 3×10^{16} and 6×10^{16}. This decrease occurs on both implanted and unimplanted samples.

The initial hypothesis was that this fluence was a critical fluence for the introduction of recombination centers into the oxide and that subsequent irradiation of this oxide would reveal reduced charge buildup over the unirradiated charge buildup curve. These samples were then annealed in two steps to remove most of the charge remaining in the oxide. Annealing was done for 10 minutes at 320°C and subsequently at 350°C for an additional 10 minutes. All charge was not removed by this process but nevertheless it appeared that most had been so that a reirradiation from these values was initiated. The hypothesis would predict that the exposure of this oxide to electron irradiation would show very little charge buildup from this point on. The experimental facts contradicted this hypothesis immeidately. As can be seen in Fig. 12 the charge buildup under positive bias after annealing was much more rapid in the thermal oxide than it had been initially. Note, for example, that on the second branch of the plot the flat band voltage under a bias of +4 volts after exposure to an electron fluence of 6×10^{13} cm^{-3} yields a flat band voltage of over 100 volts. In the initial irradiation this value was approximately 55 volts. On the other hand, the -4 volt bias curve is actually slightly less on this second branch. On the -4 volt curve at 6×10^{13} cm^{-2} the flat band voltage is 27 volts as opposed to an initial value of 45 or thereabouts. The zero bias curve is essentially the same in both branches of the plot.

The conclusion then is that the electron irradiation does influence the subsequent charge buildup behavior in the steam grown oxides but not in the manner predicted by the simple damage model initially postulated. The hypothesis that the electron beam damages the oxide similar to the ion beam is not supported. The ion beam displaces both silicon and oxygen atoms; it could be that the electron beam displaces only oxygen. This hypothesis has not been verified.

Another pertinent observation shown in a dashed line on this curve is that the value of the flat band voltage at 6×10^{16} cm^{-2} depends upon the flux of the electron beam during irradiation. If the flux is maintained at 6×10^{13} e/cm^2-sec (this is the flux value used to gather the points at a fluence of 6×10^{15} and 3×10^{16} cm^{-2}), then the value of flat band voltage does not decrease as observed initially. Instead, the flat band voltage remains at the relatively high value observed at 3×10^{16} cm^{-2}. On the initial plot the flux used to gather the last two points on this curve was 6×10^{14} e/cm^2-sec. This last observation shows that decrease in flat band voltage is flux dependent and suggests a more complicated problem in carrier kinetics. No further work was done to follow these

observations, since the conclusion reached was that this approach did not produce a less radiation sensitive oxide. The data do point out the need for improved understanding of carrier kinetics in silicon dioxide and might be useful for confirming the predictions of various models--at least qualitatively.

This change in sensitivity following exposure to high fluence electrons has been confirmed on 3 or 4 samples and appears to be a reproducible effect.

O_2^+-Implantations

Implantations using O_2^+ instead of N_2^+ were performed as part of the second implantation series. The primary objective of this experiment was to determine whether the radiation hardening property observed on the N_2^+-implanted oxides (see Figs. 8-12) depended upon the chemistry of the bombarding ion or whether the effect was primarily a physical displacement damage which could be produced by any one of a large number of bombarding particles. Problems arose in assessing wafer 6A from implantation series 2 in the sense that the metallization procedures that proved adequate for evaluating the N_2^+-implanted oxides were much less adequate when evaluating the O_2^+-implanted oxides. That this difficulty was due to a surface interaction between the implanted oxygen and the oxide is not proven but seems likely. At any rate, the net effect was that the evaporated aluminum used to make the metal electrode of the MOS capacitor failed to adhere to the O_2^+-implanted oxide nearly as well as it did to either the N_2^+-implanted thermal oxide or the straight thermal oxide. Consequently yields of acceptable and useful devices made of O_2^+-implanted thermal oxides were quite small. A few capacitors did survive and were evaluated. The small amount of data generated on these devices showed that the radiation hardening effect was similar in magnitude on the thermal oxides implanted with O_2^+ as well as those implanted with N_2^+. This conclusion must be accepted with some caution in view of the very limited number of data points on which it is based. This experiment should be repeated in the future with O_2^+ and perhaps one or two other ions.

Infrared Absorption

Wafers 1 and 2 from the first implantation series (see Table 1) were used to compare the IR absorption spectrum of the implanted oxide with an unimplanted oxide. The spectrophotometer used in this work was the Perkin Elmer 237. This is a split beam unit and in the reference path a bare

chemically etched silicon wafer was placed while the oxidized wafer was placed in the other path. Typical resulting absorption spectra are shown in Fig. 13. Curve 1 shows the absorption attributable to a 6800 Å steam-grown thermal oxide. The major features of this curve are a strong absorption in the vicinity of 9.3 microns with a lesser absorption at 12.4. These absorption bands are attributable to silicon oxygen bonds in the silicon oxide. Presumably all absorption due to the silicon substrate alone has been removed from this plot by using a silicon wafer in the reference path. Consequently, the only absorption peaks shown here should be those due to the oxide on the oxidized wafer. The silicon wafers in both cases were approximately 20 mils thick but since silicon is relatively transparent to infrared this thickness is not objectionable. The thickness of the oxide was 6800 Å, somewhat thicker than that used for the capacitance measurements described previously.

In Curve 2 the absorption characteristic of an implanted oxide is shown. The major feature of this characteristic is a slight shifting of the 9.3 absorption band and a very definite broadening in the band. This kind of a change is consistent with ruptured silicon oxygen bonds such as might be expected from displacement damage during implantation. Over the range 2.5 microns to 16 microns no additional bands or significant shifts were observed.

In Fig. 13 there is considerable oscillation obvious in the plots due most likely to the relatively rough surface finish on the oxidized samples, both the implanted and the unimplanted. The rough surfaces presumably introduce scattering and interference into the optical path which reflects itself as an oscillation. In the future specially prepared samples designed primarily for the IR measurements will eliminate this undesirable interference. Nevertheless it appears that the present spectra have revealed the major features that IR absorption measurements will show. These measurements can be extended easily to a much broader range of wavelengths.

DC Resistance, Capacitance and Dissipation Factor

Various samples were spot-checked for oxide resistance. This measurement was not part of the standard evaluation but was incorporated on certain selected implanted wafers in order to gather more information about the implantation interaction. The instrument used to make the measurements was a General Radio Corporation Megohmeter, Model 1862B. The highest value of resistance that this meter could measure reliably was 2×10^{11} ohms. In general, all capacitors exhibited dc resistance in excess of this value except those implanted at either 10^{16} N_2^+ cm^{-2} or higher or those implanted at any energy greater than 50 keV.

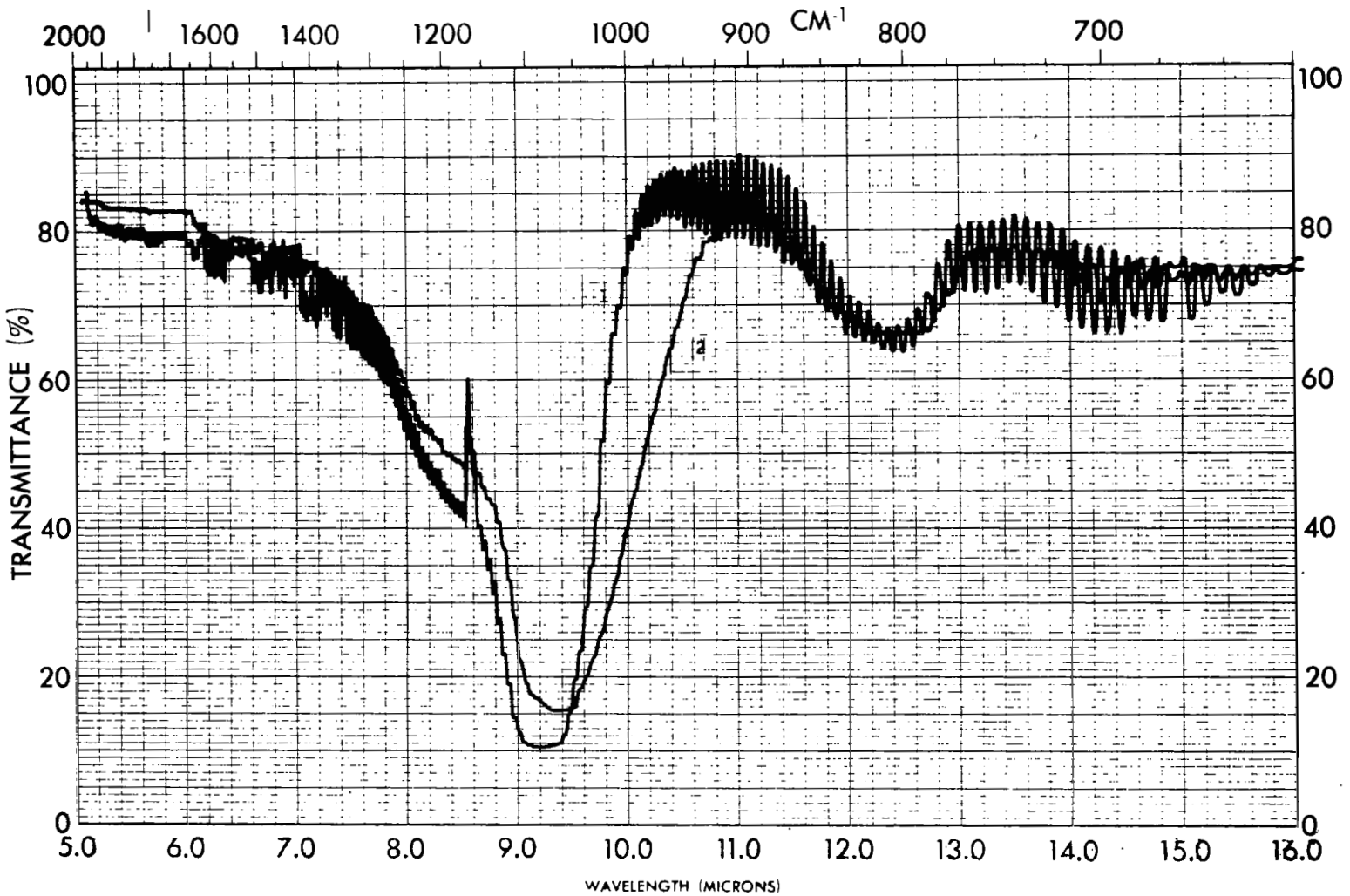

Figure 13. IR absorption spectra of: 1) steam-grown thermal oxide, and 2) implanted thermal oxide (Wafer #1).

Values of resistance measured on the 10^{16} N_2^+ cm^{-2} implanted samples (wafer 7A) were in the 10^9 to 10^{10} ohms category. This value of resistance corresponds to an oxide resistivity of 10^{11} to 10^{12} ohm-centimeters. The unimplanted oxides exhibit resistance in excess of 2×10^{11} ohms, corresponding to a resistivity greater than 2×10^{13} ohm-centimeters. Consequently, one influence of the implantation process has been to decrease the resistivity of the oxide by at least one order of magnitude and most likely two.

In general the oxide resistivity correlated with a capacitor's quality as determined by its departure from the ideal C-V curve; that is, those units which had the lowest values of resistance, 1 to 5×10^9 ohms, invariably exhibited the largest values of flat band voltage and the severest degradation in slope of the C-V characteristics.

This decrease in resistivity is not regarded as being a major objection to the implantation process. It is similar to the decrease in resistivity reported by Schmidt, et al., (Ref. 27) when in working with deposited silicon oxynitride films on silicon. Indeed the nitrogen implantation process investigated as part of this work could well produce thin layers quite similar in composition to the films investigated by Schmidt, et al. A major difference, of course, is not only the technique of deposition but the variation in composition normal to the silicon surface. In the chemical deposition technique the films presumably are constant in composition and not graded as is true for the modified thermal oxides produced by the N_2^+-implantation.

The capacitance and dissipation factor of various implanted devices (from wafer 7A, Table 2) were compared with those of their unimplanted counterparts (dry oxygen thermal oxides). The capacitance measured on the implanted and the unimplanted units were generally similar, both being in the 20 to 25 pf range (the implanted units typically exhibited 1 to 2 pf more capacitance); however, the dissipation factor measured on the implanted units typically was an order of magnitude higher. As would be expected for thermal oxides on silicon, the dissipation factor at 1 kHz was less than 0.001; after implantation, however, the dissipation factor increased to the 0.005 to 0.010 range. This increase in dissipation factor is consistent with the previously measured decrease in dc series resistance of the implanted capacitors.

All the foregoing measurements of capacitance and dissipation factor were made on a General Radio Impedance Bridge, type 1608-A, at a frequency of 1 kHz. The values quoted above are made on capacitors biased with -45 volts on the aluminum gates. Point-by-point capacitance and dissipation factor measurements were made as a function of bias over a limited range. For the implanted wafers the dissipation factor exhibited a maximum in the vicinity of -5 volt bias on the aluminum gate. The peak in dissipation factor for the nonimplanted oxides occurred closer to 0 volt bias.

After 20 keV electron irradiation, the peaks in the dissipation factor occurred at larger biases, were broader, and were greater in magnitude. At biases below the flat band voltage the magnitudes of the dissipation factor for both the implanted and the unimplanted units were in the 0.2 to 0.3 range. When biased to a value above the flat band voltage, the dissipation factor of the unimplanted units returned to a value less than 0.001. The implanted units, on the other hand, remained at a value somewhat above their pre-electron irradiation value in the 0.01 to 0.02 range.

Etch Rate

Comparative measurements of the etch rate of the implanted oxide with the unimplanted oxide were carried out on wafer 1 (see Table 1). This wafer was implanted so as to exhibit a readily recognizable region of different color along the horizontal diameter of the wafer during implantation. The altered color of the implanted region was ascribed to an altered index of refraction for the implanted region. No independent confirming measure of the index of refractive was made, however.

The composition of the etch used initially to measure comparative etch rates was:

15 cc HF (48%)
10 cc HNO_3 (70%)
300 cc H_2O

This is the P-etch developed by Pliskin of IBM as a highly discriminating etch between silicon dioxide and other glass compositions rich in silicon oxide. The P-etch rate of thermally grown silicon oxide on silicon is approximately 2 Å/sec.

When wafer 1 was etched in P-etch, the implanted region was not visibly attacked after 1 hour and 15 minutes. The unimplanted oxide surrounding the implanted region was attacked and etched at about 3.5 Å/sec at the wafer edge. Closer in toward the implanted region the etch rate was faster, suggesting that the number of ions striking this area was greater than at the wafer edges but not great enough to cause the color changes characteristic of the center implanted region. Enhanced etch rate caused by ion bombardment has been previously observed (Ref. 28). This action could explain the faster oxide etching of the oxide near the heavily implanted region. The heavily implanted region, however, did not etch at all but remained as a fairly sharply defined region in the center of the wafer.

Buffered HF--10 cc HF (48%), 100 cc NH_4F soln. (1 lb. NH_4F/680 cc H_2O)--did not attack the implanted region either. Concentrated HF (48%)

attacked the region preferentially, leaving small islands of the implanted layer unaffected but removing most of the region. The appearance of the heavily implanted region after 15 minutes in HF suggested preferential attack along defects or damage channels which undercut the surface oxide. The observations were consistent with an insoluble surface layer on a soluble base as though the chemical etch of the base layer began at a finite number of discrete pinholes or defects in the insoluble surface layer. The etch proceeded radially from these points removing the insoluble surface layer by undercutting.

EVAPORATED OXIDES

Previous work published by other investigators has shown that the radiation sensitivity of oxides prepared by evaporation from a silicon monoxide source have been very radiation insensitive (Refs. 8,18). Unfortunately these oxides have been far less stable electrically than the standard thermally grown silicon dioxide layer and hence have not been very useful. The purpose of this investigation was to develop some modification which might permit these oxides to be prepared in such a fashion that they would retain their desirable radiation insensitivity but display much improved electrical stability.

Apparatus

The basic vacuum system in which these evaporated oxides were prepared was an ion pumped vacuum chamber manufactured by the Ultek Corporation. The silicon monoxide powder used for this work was rated mesh 30 and supplied by the R. D. Mathis Company. Prior to evaporation no cleaning or other processing of the material was carried out; it was loaded directly into a SiO evaporation furnace. This furnace consists of a refractory metal shaped so as to be a baffle and a heating element. The silicon monoxide is contained in this furnace in such a position that no direct line of sight exists between it and the substrate to be coated. In order for evaporation to occur the silicon monoxide must first be vaporized and then by collision and reflection from the various baffles of the furnace find the exit path. This arrangement is necessary in order to avoid large chunks of SiO powder spewing off and depositing as a meteor on the substrate surface.

The silicon substrate to be coated was positioned approximately 6 inches above the SiO furnace and was suspended by pencil tweezers. The tweezers themselves were attached to an arm which could be pivoted from one section of the vacuum chamber (that section containing the SiO furnace) to another section in which the metallization could be deposited

on the evaporated oxide layer. The temperature of the silicon substrate was not controlled during evaporation but because of the relatively low thermal mass of the silicon, the radiant energy from the silicon monoxide furnace probably succeeded in heating it to an excess of 100°C.

The evaporation rate was maintained at 1 Å per second. The thickness of the deposited film was monitored continuously by a mass monitor manufactured by Sloan Instrument Company. This mass monitor consists of an oscillating quartz crystal which is water cooled to avoid the undesirable effects of temperature that such quartz crystal oscillators are subject to. The procedure used to establish evaporation rate was to commence the evaporation at nominal power settings on the SiO furnace, record the film thickness at a sequence of times (actually the voltage signal corresponding to the film thickness was plotted on a recorder so that thickness as a function of time was recorded permanently). From this record small corrections to achieve the desired slope could be readily made and when the slope approached the desired value of 1 Å per second, the silicon wafer was moved into the evaporating stream. The time required to place the wafer in the proper position was small compared to the total evaporation time--typically the time required to position the wafer from completely out of the evaporating beam to a stable position within it was on the order of 5 seconds, while the total time of the evaporation was on the order of 2000 seconds. Once the desired film thickness had been reached at the desired rate the wafer was rotated out of the SiO stream and positioned in a shielded position midway between the SiO source and the aluminum source set up adjacent to the SiO source.

The aluminum was deposited at a relatively high rate (40 Å/sec) and was heated by an electron gun. As with the thermally grown oxides, the aluminum was deposited through a metal mask consisting of an array of 15 mil holes on 20 mil centers. After melting and commencing the evaporation with the silicon wafer in a shielded position, the power to the electron gun was reduced and the silicon wafer was moved into a position above the molybdenum mask and dropped snuggly down against it. The power to electron gun was then reapplied to complete the evaporation.

Here as in all previous structures evaluated, the oxide thickness was 2000 Å and the metallization thickness on top of the oxide was 1000 Å.

With this vacuum arrangement and fixturing the preparation of MOS capacitors could be carried out with 1 pumpdown. The only remaining steps of fabrication consists of wafer bonding and wire bonding in order to have a unit ready for test.

Results

Evaporated layers of oxide were put down on various substrates. Among them were bare silicon surfaces (this is a silicon surface which has been chemically etched to expose a fresh silicon surface but then

subsequently cleaned in oxidizing acids to form a thin oxide layer on the order of 20-50 Å) and silicon wafers covered with thin thermal oxides of various thicknesses. The results for all these samples were the same--instabilities due to contamination dominated the observed C-V properties and rendered further development unattractive. The influence of the contaminants will be emphasized in the following paragraphs.

At room temperature the C-V characteristic of an evaporated oxide on silicon is illustrated in Fig. 14. The hysteresis evident in Fig. 14 is typical of a structure showing charge injection, since negative bias on the aluminum electrode (or positive bias on the silicon electrode) has the effect of increasing the positive charge in the oxide. This action is the reverse of what would be expected with ion motion in the oxide. Placing a negative bias on the aluminum gate attracts positively charged ions in the oxide and pulls them further away from the oxide-silicon interface. This shift in position in the oxide makes these positive ions less effective electrostatically at the oxide-silicon interface so that the C-V curve approaches the ideal curve more closely after such a bias stress. For those samples prepared from silicon monoxide evaporated onto a bare silicon substrate, this type of instability is reversed--placing a negative bias on the aluminum gate has the effect of making the C-V characteristic less ideal--as though the magnitude of the

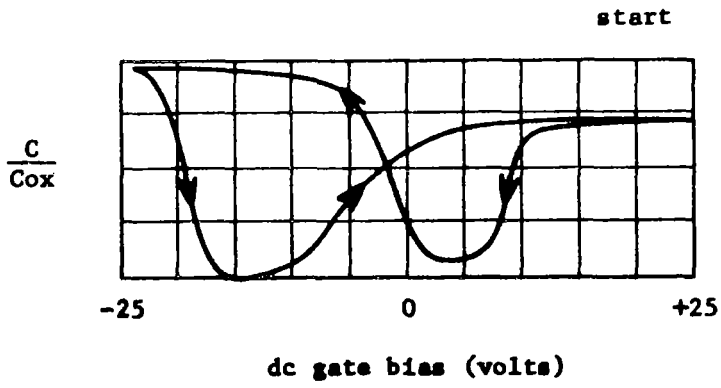

Figure 14. Hysteresis in the C-V characteristics of an oxide evaporated from a silicon monoxide source. The dc bias begins at +25 V, proceeds to -25 V at 2 volts/sec, immediately reverses, and returns to +25 V at the same sweep rate.

positive charge near the oxide-silicon interface is greater after such bias exposure rather than less. Simply postulating that the dominant ion is a negative ion does not explain the observations, for while it is true a negative ion would be drifted toward the oxide-silicon interface with negative bias on the aluminum gate, a buildup of negative charge at the oxide silicon interface would shift the C-V curve in closer to the ideal characteristic as well. This conflicts with the observations. Consequently the model usually invoked to explain the type of instability observed here is charge injection across the oxide-silicon interface. This charge injection could be hole injection from the silicon into the oxide or electron injection from the oxide into the silicon. It changes rapidly with bias as can be seen from the hysteresis evident in the C-V characteristic (Fig. 14).

By inserting a thin oxide layer between the evaporated oxide and the silicon the direction of the instability changes as shown in Fig. 15. At room temperature the C-V curves display large instabilities very similar to those shown in Fig. 14 but the direction or bias dependence of this instability is reversed. Here a negative bias on the aluminum gate displaces the flat band voltage to the right--as though negative charges were being added to this silicon dioxide. In fact, the curves shift so far to the right as to reflect a total net negative charge in the oxide. This observation is consistent with the presence of negative ions in the oxide and has been observed with our evaporated oxides on top of thermal oxides.

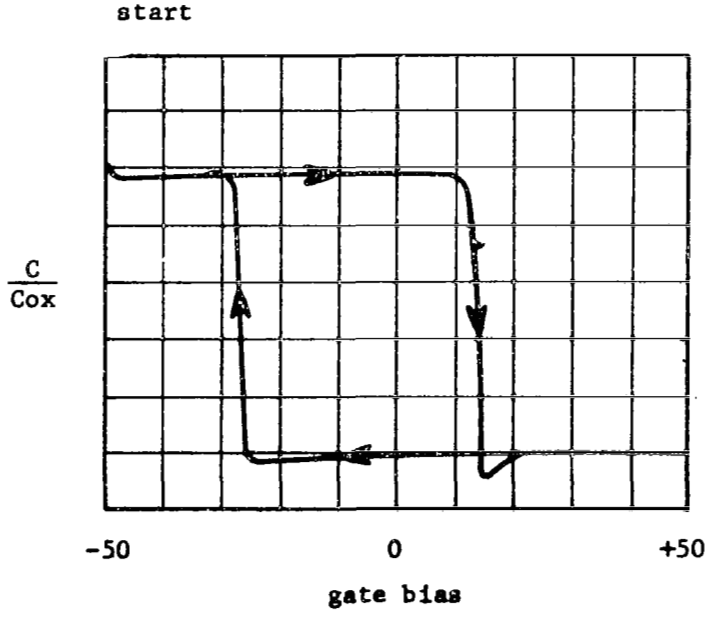

Figure 15. C-V properties of sample E-2. This trace was made by starting the bias at -50 V, proceeding to +50 V at 2 volts/sec, remaining at +50 V for 1 minute and returning to -50 V at 2 volts/sec. sweep.

Even on samples containing no thermal oxide the effect of ions can be seen to dominate the characteristics as shown in Fig. 16. This shows a structure at 40°C biased positively at 25 volts. The initial characteristics show a flat band voltage of approximately -8 volts. After 1 minute under bias the flat band voltage has shifted toward the right to a value of -2 volts or thereabouts. Ten minutes later the curve under the same bias has shifted back toward the left indicating that the ion motion is now dominating the characteristic. Further bias shifts the curve far to the left showing that ions are dominating the characteristic completely even though the initial displacement was consistent with that of charge injection.

The inability to remove the effects of ions in these oxides prevented the gathering of meaningful irradiation data. Some irradiations were attempted but in all cases the instabilities due to voltage biases were far greater than any instabilities or shifts in properties brought about by the irradiation itself. In carrying out these irradiations the structures containing evaporated oxides were found to be very fragile. This statement applies primarily to the evaporated oxides on bare silicon but also to a lesser degree to evaporated oxides on the thin thermal oxides on silicon. The yields across a given wafer for the former averaged about 50% satisfactory capacitors. Upon placing these capacitors into the vacuum system for electron irradiation, however, all the remaining satisfactory capacitors degraded in dissipation factor and dc resistance

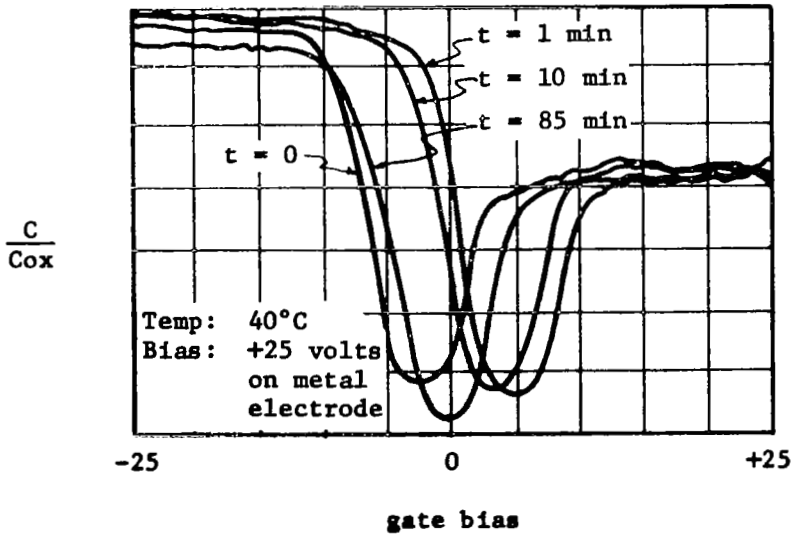

Figure 16. Bias-temperature behavior of E-1. Note reversal of flat band voltage shift after t = 1 min.

until they were no longer useful. This degradation was before any electron irradiation and appeared to be caused by the vacuum pumpdown operation alone. The interaction is not understood at present and was not pursued because of the contaminant-caused, unstable electrical properties of these capacitors. The action could be described, however, as that of a low power dissipation, one-time switch. The units are good capacitors in the atmosphere but upon being exposed to a vacuum they degrade electrically but not in such a fashion as to draw much power.

Those units containing a thin layer of thermally grown oxides between the evaporated oxide and the silicon were somewhat more rugged and did survive some electron irradiation. However, the fluence that these units could be tested at before failing catastrophically as capacitors was relatively low.

CONCLUSIONS AND RECOMMENDATIONS

Two methods were investigated for improving the radiation resistance of thermal oxides on silicon: 1) ion implantation, and 2) evaporation of SiO. The more promising by far was that in which the properties of the thermal oxide were modified by an ion implantation process. This approach to radiation hardening retains all the advantages of the well established and highly perfected techniques of thermal oxidation and requires only the degradation of a specific property--the electron lifetime in the oxide. Preliminary work has been carried out with an N_2^+ ion beam and it has been shown that all thermal oxides investigated have been improved in radiation hardness by this modification. Most of the work of this investigation was carried out on implantations which were sufficiently high in fluence so as to introduce a small shift into the initial C-V characteristic of the MOS capacitor structure used for evaluating the modification. The magnitude of this shift is small compared to the improvement in radiation hardness and does vary with fluence. It is by no means certain that the optimum ion, fluence, or range (energy) have been identified as yet. What has been shown is that ion implantation can modify the properties of an oxide and among the desirable modifications that implantation can bring about is that of radiation hardening.

Evaporated oxides were also investigated but the inability to produce these oxides without contaminating ions led to abandoning this effort early in the program.

Three general tasks should be further explored or initiated: 1) the development of better understanding of the physics of the ion implantation-induced modification. Most of the observations to date suggests that displacement alone could be responsible for the radiation hardening effect. If this is true then annealing cycles might eliminate

the effect; investigation of such annealing parameters is an important future experiment. Chemical effects have also been identified and examination of their significance should also be continued. 2) Development of an optimum modification process. The better understanding developed by Task 1 should point the way to the optimum method for implementing the modification process in the future. Optimization should include not only efficiency of the modification but the economy and ease of the modification as well. If other bombarding species are more efficient or more readily available, they should be given preference over the already investigated nitrogen and oxygen ions. 3) The fabrication of MOS field effect transistors utilizing the modified oxide developed in Task 2 and a comparison of the properties of these units with their counterparts built with oxides not so modified.

REFERENCES

1. Kahng, D.; and Atalla, M. M.: Silicon-Silicon Dioxide Field Induced Surface Devices. Presentation at Solid State Device Research Conference, Pittsburgh, Pa., June 1960.

2. Sah, C. T.: A New Semiconductor Tetrode--the Surface Potential Controlled Transistor. Proc. IRE, vol. 49, Nov. 1961, pp. 1623-1634.

3. Sah, C. T.: Characteristics of the Metal-Oxide-Semiconductor Transistors. IEEE Trans. Electron Devices, vol. ED-11, July 1964, pp. 324-345.

4. Hofstein, S. R.; and Heiman, F. P.: The Silicon Insulated-Gate Field Effect Transistor. Proc. IEEE, vol. 51, Sept. 1963, pp. 1190-1202.

5. IBM Journal of Research and Development, vol. 8, Sept. 1964, pp. 365-480.

6. Hughes, H. L.; and Giroux, R. R.: Space Radiation Affects MOS FETS. Electronics, vol. 37, Dec. 1964, pp. 58-60.

7. Deal, B. E.: (to Fairchild Camera and Instrument Corp.), Method of Making Stable Semiconductor Devices. U.S. Patent 3,426,422, Feb. 11, 1969.

8. Snow, E. H.; Grove, A. S.; and Fitzgerald, D. J.: Effects of Ionizing Radiation on Oxidized Silicon Surfaces and Planar Devices. Proc. IEEE, vol. 55, July 1967, pp. 1168-1185.

9. Zaininger, K. H.: Electron Bombardment of MOS Capacitors. Appl. Phys. Letters, vol. 8, no. 6, March 15, 1966.

10. Mitchell, J. P.: Radiation-Induced Space Charge Buildup in MOS Structures. IEEE Trans. on Electron. Devices, vol. ED-14, no. 11, Nov. 1967, pp. 764-774.

11. Simons, M.; Montieth, L. K.; and Hauser, J. R.: A Study of Charge Storage in Silicon Oxide Resulting from Non-Penetrating Electron Irradiation. NASA CR-1088, June 1968.

12. Dennehy, W. J.; Holmes-Siedle, A. G.; and Zaininger, K. H.: Process Techniques and Radiation Effects in Metal-Insulator Semiconductor Structures. IEEE Trans. on Nucl. Sci., vol. NS-14, no. 6, Dec. 1967, pp. 276-283.

13. Grove, A. S.; and Snow, E. H.: A Model for Radiation Damage in Metal-Oxide-Semiconductor Structures. Proc. IEEE (letters), vol. 54, June 1966, pp. 894-895.

14. Williams, R.: Photoemission of Electrons from Silicon into Silicon Dioxide. Phys. Rev., vol. 140A, Oct. 1965, pp. A569-A575.

15. Revesz, A. G.; Zaininger, K. H.; and Evans, R. J.: Reduction of Radiation Sensitivity in MOS Structures by Aluminum Doping of Silicon Dioxide. J. Electrochem. Soc., vol. 116, Aug. 1969, pp. 1146-1148.

Lindmayer, J.; and Noble, W. P., Jr.: Radiation Resistant MOS Devices. IEEE Trans. Electron Devices, vol. ED-15, Sept. 1968, pp. 637-640.

16. Perkins, C. W.; Aubuchon, K. G.; and Dill, H. T.: Radiation Effects in Modified Oxide Insulators in MOS Structures. IEEE Trans. Nucl. Sci., vol. NS-15, Dec. 1968, pp. 176-181.

17. Zaininger, K. H.; and Waxman, A. S.: Radiation Resistance of Al_2O_3 MOS Devices. IEEE Trans. Electron Devices, vol. ED-16, April 1969, pp. 333-338.

18. Hughes, H. L.: Comparative Study of Ionizing Radiation Surface Effects Utilizing MOS Devices Fabricated with Various Dielectrics. IEEE Conf. on Nucl. and Space Radiation Effects, Stanford, Calif., July 1966.

19. Grove, A. S.; Deal, B. E.; Snow, E. H.; and Sah, C. T.: Investigation of Thermally Oxidized Silicon Surfaces using Metal-Oxide-Semiconductor Structures. Solid State Electron., vol. 8, Feb. 1965, pp. 145-163.

20. Zaininger, K. H.: Semiconductor Surface Physics. Field Effect Transistors, J. T. Wallmark and H. Johnson, eds., Prentice-Hall, Inc., 1966, pp. 17-56.

21. Nicollian, E. H.; and Goetzberger, A.: MOS Conductance Technique for Measuring Surface State Parameters. Appl. Phys. Letters, vol. 7, Oct. 1965, pp. 216-219.

22. Nicollian, E. H.; and Goetzberger, A.: Electrical Characterization of the $Si-SiO_2$ Interface by the MIS Conductance Technique. Bell System Tech. J., March 1967.

23. Lindhard, J.; Scharff, M.; and Schiott, H.: Range Concepts and Heavy Ion Ranges. Mat. Fys. Medd. Dan. Vid. Sclsk, vol. 33, 1963, pp. 1-39.

24. Gibbons, J. F.: Ion Implantation in Semiconductors-Part I, Range Distribution Theory and Experiments. Proc. IEEE, vol. 56, no. 3, March 1968, pp. 295-319.

25. Gray, P. V.; and Brown, D. M.: Density of SiO_2-Si Interface States. Appl. Phys. Letters, vol. 8, no. 2, Jan. 1966, pp. 31-33.

26. Burger, R. M.; and Donovan, R. P., eds.: Fundamentals of Silicon Integrated Device Technology, Vol. 1 Oxidation, Diffusion and Epitaxy. Prentice-Hall, Inc., 1967, p. 28.

27. Schmidt, P. F.; Rand, M. J.; Mitchell, J. P.; and Ashner, J. D.: Radiation-Insensitive Silicon-Oxynitride Films for Use in Silicon Devices. IEEE Trans. Nucl. Sci., Dec. 1969.

28. Roosild, S.; Dolan, R.; and Buchanan, B.: Annealing Studies of Damage Introduced by High Energy Ion Implantations of Silicon. Presentation to the 1969 IEEE Annual Conference on Nuclear and Space Radiation Effects (University Park, Pa.), July 8-11, 1969.

NASA-Langley, 1970 —— 26 CR-1584